INFORMATION TO USERS

This manuscript has been reproduced from the microfilm master. UMI films the text directly from the original or copy submitted. Thus, some thesis and dissertation copies are in typewriter face, while others may be from any type of computer printer.

The quality of this reproduction is dependent upon the quality of the copy submitted. Broken or indistinct print, colored or poor quality illustrations and photographs, print bleedthrough, substandard margins, and improper alignment can adversely affect reproduction.

In the unlikely event that the author did not send UMI a complete manuscript and there are missing pages, these will be noted. Also, if unauthorized copyright material had to be removed, a note will indicate the deletion.

Oversize materials (e.g., maps, drawings, charts) are reproduced by sectioning the original, beginning at the upper left-hand corner and continuing from left to right in equal sections with small overlaps.

ProQuest Information and Learning
300 North Zeeb Road, Ann Arbor, MI 48106-1346 USA
800-521-0600

Experimental Investigation of Vehicle's Lateral Acceleration on Highway Horizontal Curves

Submitted by

Liaquat Syed

A thesis submitted to the Faculty of Graduate Studies and Research in partial fulfillment of the requirements for the degree of Master of Applied Science

Department of Civil and Environmental Engineering

Carleton University

Ottawa, Ontario

The Master of Applied Science and Civil Engineering is a joint program with the University of Ottawa, administered by the Ottawa-Carleton Institute of Civil Engineering

Abstract

It is documented in the literature that the speeds selected by drivers on left-turn curves were higher than the speeds on the right-turn curves. The data collected from seventy curves of two-lane rural highways located in Eastern Ontario Canada for this research also showed the trend of higher values of lateral acceleration on right-turn curves compared to left-turn curves. This thesis further explains the previous findings by going in depth with the reason why the lateral acceleration is lower on left-turn curves. A subsequent objective of this research is to develop models for prediction of lateral acceleration with uneven weight in the vehicle. Turning direction coupled with uneven weight distribution in a vehicle significantly affects the values of lateral acceleration during curve driving. If a vehicle –with extra weight on the driver side- is turning right on a superelevated curve, the excess static weight will generate a feeling of more lateral force as indicated in a greater lateral acceleration, compared to a left-turn. This difference in the lateral acceleration values could result in different driving speeds on left-turn and right-turn curves.

Acknowledgments

I would like to express my sincere appreciation to my thesis supervisor Prof. Yasser Hassan, of the Department of Civil and Environmental Engineering, Carleton University for his guidance and help in completing this study.

I also like to express my gratitude to Prof. Robert G. Langlois of Department of Mechanical and Aerospace Engineering, Carleton University for his sincere guidance. I am also thankful to the Staff of Civil Engineering Laboratory for their support.

Table of Contents

List of Tables

List of Figures

Chapter 1
Introduction

1.1 Background

In early 1900's, the motorized vehicle appeared, and mass production for the general public started in the 1920's with top speeds over 50 miles per hour. Almost overnight, the system of roads and trails had to be re-developed to accommodate these vehicles. Road surfaces had to be hard, paved, and dust proof, to serve the higher speeds (Merritt 1988).

The motorized traffic brought tremendous changes in mobility, which transformed almost every quarter of human life. On one hand, it increased the economical growth rates, and on the other hand it became one of the major reasons of fatalities during accidents and economical losses owing to accidents and gridlocks on roads.

Highway accidents killed more than 42,000 Americans and injured another 3 million in the year 2001 alone. Generally, one crash occurs every 5 seconds, and more than 4,900 pedestrians lose their lives in traffic crashes every year on highways in the United States of America alone (Leiphart 2002).

In the member countries of the Organization for Economic Co-operation and Development (OECD) -a group of 28 mostly developed countries- approximately 125,000 people die on the roads every year (OECD 2002). In other words, one road crash victim dies every four minutes. In 1990, road crashes were ranked as the ninth largest disease or injury burden in the world. Furthermore, a study co-sponsored by the World Bank, Harvard University and the World Health

Organization, predicted that road crashes will represent the third largest burden by the year 2020, exceeded only by heart disease and depression (OECD 2002). In comparison, wars will be the eighth highest cause of death, while HIV will be the tenth. The most regrettable fact is that a large number of road fatalities and causalities are not an inevitable result of motorization, and to a large degree many are preventable.

In addition to the devastating impacts on human life, vehicle crashes also impose substantial economic costs on the society. In 1926, when researchers first began studying the impacts of vehicle crashes in the USA, economists estimated that the direct and indirect costs due to traffic collisions were approximately $600 million per year. Furthermore, another $2 billion per year losses occurred due to congestion and lost productivity. By the year 2001, the annual economic cost of traffic crashes had risen to $230 billion in America alone (Leiphart 2002).

Highway curves are necessary elements of all highways. Despite reasonably well-conceived design procedures, highway curves continually show a tendency to be high-accident locations. The average accident rate for highway curves is about three times higher than that for highway tangents, while single-vehicle run-off-road accident rate is about four times higher on highway curves (Glennon 1987).

One of the important factors of curve driving is the perception of the lateral force, which results from a change in the direction of motion. Lateral acceleration is generated as a vehicle negotiates a horizontal curve with a constant radius

and is counterbalanced by a combination of a vehicle weight component related to the roadway superelevation and side friction developed between the tires and pavement surface (Carlson and Mason 1999).

1.2 Problem Definition

Driving speeds and the corresponding lateral accelerations experienced on curves on wet and dry pavements are points of particular interest in curve driving. Glennon et al. (1983) reported that the best explanation of the car-driver behavior is the lateral acceleration because it is felt by the driver and passengers and at the same time affects the tire-pavement friction forces.

Lateral acceleration comprises the physical output of the different variables for driving on a horizontal curve. Some investigators – such as Ritchie et al. (1968), Kneebone (1964), and Moyer and Berry (1940) - measured the values of the lateral acceleration of vehicles on curves.

Researchers have presented several concerns regarding the American Association of State Highway and Transportation Officials (AASHTO) guidelines for horizontal curve design. Specifically, the maximum design side friction factors recommended by the AASHTO Green Book are considered at the upper limits of motorist comfort. The first issue related to these limits is that they are based on studies conducted in 1920 to 1952, while today's drivers have possibly become more tolerant of lateral acceleration due to changes in attitude and vehicle cornering capabilities. The second issue raised is regarding the relationship between the design speeds and unbalanced lateral acceleration. In a review of unbalanced lateral acceleration recommended by twelve international highway

agencies, differing opinions were found about the level of unbalanced lateral acceleration suitable for a given speed (Bonneson 2001).

Therefore, while looking at the entire issue of curve driving from the lateral acceleration prospective, there is still a need to further investigate its relationship with other features of curve driving. This is particularly true in Canada, as very few studies have been conducted in this country. As such, there is no clear picture of the levels of lateral acceleration and side friction suitable for Canadian driving conditions where there are different weather conditions and posted speed limits.

1.3 Objectives

The general objectives of this thesis are to provide a detailed review of the relationship between lateral acceleration and other related components of highway curves and vehicle dynamics as well as to compare the values of lateral acceleration collected through two different types of equipment. More specific objectives of this study include:

- Comparing the lateral acceleration values of the vehicle with uneven weight distribution on left-turn curves to right-turn curves.
- Comparing lateral acceleration calculated by using the analytical model available in the design guides (theoretical lateral acceleration) and lateral acceleration measured (observed lateral acceleration) in the field.

- Examining the relationship between produced actual lateral accelerations based on curve parameters and driving speeds of the curves.
- Developing models for prediction of lateral acceleration with uneven weight distribution in the vehicle.

1.4 Thesis Structure

This thesis consists of six chapters. Chapter 1 focuses on the background, problem definition and objectives of the study. Chapter 2 provides a review of the literature already available on the issues being discussed in this study. Chapter 3 describes the procedure and strategy adopted for data collection and introduction to the equipment used in this study. Chapter 4 presents the efforts related to processing of collected data. Chapter 5 deals with analysis of the data including its comparison with previous work, and models development. Chapter 6 includes the conclusions and recommendations submitted. References are also provided at the end of the thesis.

Chapter 2
Literature Review

One of the most important parts of any study is to acquire complete information of the work already done prior to the study in hand. Therefore, a thorough literature review was carried out on curve driving involving lateral acceleration. This review helped reach a better understanding of the work done so far and also led to the gaps in the research where further studying is required.

Roads are rarely straight and level. Rather, they include such features as curves and gradients, and therefore vehicle speeds are dependent upon road geometrics. Geometric elements of a highway curve such as radius, superelevation rate, and side friction factor are meant to provide safe and continuous traffic flow. Forces developed on a vehicle moving on a circular highway curve due to lateral acceleration are inversely proportional to the radius of curve and directly proportional to the square of driving speed. It is counterbalanced by a combination of the vehicle-weight component related to the roadway superelevation and the side friction developed between the vehicle tires and pavement surface. This chapter deals with the description of fundamentals of different features of curve driving and vehicle dynamics. The relationships between these features and developed models are also described.

2.1 Curve Radius

Among the current AASHTO criteria for horizontal curve design is to choose the radius and superelevation so that lateral acceleration felt by the occupants of vehicle traversing the horizontal curve of highway is kept within comfortable

limits (Carlson and Mason 1999). The model given below is used by AASHTO guidelines to determine the minimum radius of curve for a specified superelevation. This model is commonly known as the point-mass equation:

$$f + e = V^2/(127R) \qquad (2.1)$$

where

f = side friction factor

e = superelevation rate (m/m)

V = speed of vehicle (km/h)

R = radius of curve (m)

A strong relationship between the radius of a curve and accident occurrence has been recognized for quite some time. An early study of the relationship between accidents and highway design features showed that as the radius of a horizontal curve decreased, the accident rate increased (Baldwin 1946). A study conducted by Lamm et al. (1991) provided more evidence of this relationship by using data from 197 curves in New York State as shown in Table 2.1.

Table 2.1: Relationship Between Degree of Curve and Accident Rate (Lamm et al. 1991)

Degree of Curve	Average Accident Rate (Acc./Million veh-miles)	Change in Operating Speed (km/h)	Significance (at 95% confidence level)	Remarks
Tangent	1.87	No Change		
1° - 5°	3.66	Up to 10	Yes	Good Design
> 5° - 10°	8.05	10 to 20	Yes	Fair Design
>10°- 15°	17.55	> 20	Yes	Poor Design
>15° -26.9°	26.41	> 20	Yes	Poor Design

Felipe and Navin (1998) evaluated the validity of different basic variables involved while driving through a horizontal curve. They found that radius of curve is very influential in the selection of driving speed on horizontal curves. In their study, they measured the actions of automobile drivers on horizontal curves of an abandoned runway and a two-lane rural highway located in British Columbia, Canada. Independent variables considered were: speed (comfortable and fast), pavement surface (dry and wet), gender (male and female), and curve radius (16, 26, 60 and 100 m)

The outputs measured were the driver's selected speed, corresponding lateral acceleration and passenger's comfort level. Tests were carried out on hot sunny days by driving a midsize sedan. An 8-mm video camera mounted on the right rear side window, pointed down at equally spaced and marked curve pavement was used for calculating the speed through a certain period of time over distance between two marks. A "g-analyst" type accelerometer included a

three-axis acceleration transducer unit was used on the floor between the driver and the passenger and between the front and rear seats.

The data indicated that the variation in the speed of the test vehicle was influenced by change of speed between comfortable (drive the curve at such a speed that driver feel comfortable) and fast speed scenario (drive the curve at the maximum speed that driver consider to be safe) and change of radius. On the small radii, the test subjects reduced their speed to a minimum at approximately the centre of the curves; then they accelerated toward the exit. This phenomenon was observed for both comfortable and maximum safe speed scenarios, but was not observed for the large radii.

2.2 Superelevation

In the early days of motor vehicles, most common accidents were run-off road and head-on collisions. At that time, there was little or no uniformity in the highway engineering practice. In case of long tangent sections, vehicles speeds were as high as the vehicle's capability could allow, and drivers were expected to slow down on curved portions. The amount a driver would slow down was an independent decision based on judgment and experience. Misjudgment of the drivers was the reason for much of the collisions (Merritt 1988).

The concept of balanced design was, proposed in the early 1930's to increase the chances for a driver to safely traverse the curved section of highway with the same speed as the tangent portion (Merrit 1988). Road designers in the 1920's and 1930's were those who started their careers as railroaders. They first introduced the concept of superelevation from the practice of banking one rail on

a curved portion. The purpose was to counteract the outward forces and make it possible for railroad cars to travel at about the same speed on the curve and straight portion. This effect was applied in the road design by the name of superelevation (Merritt 1988).

Fitzpatrick (1994) in her study stated "when a vehicle moves on circular path, it is forced radially outward by centrifugal force. Superelevation is the rotation of the roadway cross section to offset the centrifugal force acting on a vehicle traversing a curved section. For each combination of curve radius and travel speed, there is a specific superelevation that will precisely balance the centrifugal force. When a vehicle travels at speeds greater than those at which the superelevation can balance all of the centrifugal force, side friction is needed to keep the vehicle on the curved path".

A curve with a minimum radius needs superelevation and side friction factor at their maximum values. While in case of very flat radii, a normally sloped cross-section may be adequate and superelevation may not be needed. In between these two positions, centripetal acceleration needed to track the curve is satisfied using both the side friction and superelevation (Bonneson 2001).

Several methods are available for distributing superelevation and side friction over a range of curves. The AASHTO (2001) guidelines for design of superelevation list five methods:

1. Superelevation rate is directly proportional to the degree of curvature i.e. superelevation rate varies from zero to maximum when radius of curve value is infinity (∞) to minimum, respectively.

2. Counteracting the centrifugal force with friction up to the maximum friction and then using a straight-line relation, increasing superelevation as the curvature increases up to maximum superelevation;
3. Counteracting the centrifugal force with superelevation only until maximum superelevation is reached and then using a straight-line relation, increase friction as the curvature increases up to maximum friction;
4. Same as the previous method, except that this method is based on average running speed instead of design speed, and
5. There is a curvilinear relationship between superelevation and side friction.

Bonneson (2001) extensively worked on the issues related to the relationship between superelevation rate and curve design and stated that "the minimum superelevation rate based on 95th percentile drivers should be the rate necessary to ensure that side friction demand of the majority of drivers is not excessively large". It was found that excessively high side friction demand reduced margin of safety and caused large speed reduction on curve entry. He further explained, "the maximum superelevation rate suitable for curve design should be the rate necessary to ensure that the side friction demand of the majority of drivers is not very small". As negative side friction demand requires drivers to steer in the opposite direction of the curve, which is logically unsafe. He found that some of the superelevation rates recommended in the AASHTO (2001) guidelines may subject slower drivers to negative side friction demands especially in case of lower design speeds. A similar problem may occur for larger

maximum superelevation rates at higher design speeds. This problem might create two deficiencies in AASHTO's superelevation distribution methods listed earlier in this section.

1. It violates the maximum superelevation rate based on the 5th percentile driver control under some conditions.
2. Use of separate distribution curves for each design speed and maximum superelevation rate leads to violations in design consistency.

Bonneson (2001), in his efforts to resolve these two deficiencies, proposed a superelevation distribution method based on the two models given below (Equation 2.2 and 2.3).

$$e_d = e_{\max}\{R_{\min} / R\} \tag{2.2}$$

with

$$n = \{\ln(-0.01e_{NC}) - \ln(0.01e_{\min}\}/\{\ln(R_{\min}) - \ln(R_{NC})\} \tag{2.3}$$

where

e_d = design superelevation rate (percent)

$e_{\max}$ = maximum superelevation rate (percent)

R = radius of curve (m)

$R_{\min}$ = minimum radius with maximum superelevation rate (m)

e_{NC} = cross slope rate in section with normal cross slopes

n = shape factor

$e_{\min}$ = minimum superelevation rate (percent)

R_{NC} = curve radius with normal cross slope (m)

$\ln(x)$ = natural log of x

2.3 Lateral Acceleration

An important outcome of driving is the perception of the lateral force, which results from a change in the direction of motion. It is not yet clear to what extent this kinaesthetic perception is related to visual perception. The safe driving on curves at high speeds may depend strongly on the interaction between these two senses. Drivers by their habit choose the speed at which they will negotiate a curve before entering the curve. If the curve is new to them, this choice must be based on visual perception (Ritchie et al. 1968).

2.3.1 Definition

When a particle moves in a circular path of constant radius with constant speed, it generates centripetal acceleration, directed toward the centre of the circle, perpendicular to the instantaneous velocity (Equation 2.4):

$$a_c = v^2 / R \qquad (2.4)$$

where

a_c = centripetal acceleration (m/s^2)

v = speed of vehicle (m/s)

R = radius of horizontal curve (m)

As per Newton second law of motion ($F = ma$), the above-mentioned acceleration must be caused by a force also directed toward the centre of the

curve. The net radial force on a vehicle of mass "m" travelling in uniform circular motion is:

$$F = ma_c = mv^2 / R \qquad (2.5)$$

where

F = net radial force (N=kg-m/s^2)

m = mass of vehicle (kg)

The centripetal acceleration (refer to Equation 2.4) is known as lateral acceleration in highway engineering. Carlson and Mason (1999) in their study stated that "lateral acceleration is generated as a vehicle negotiates a horizontal curve with constant radius and is counterbalanced by the vehicle weight component related to the roadway superelevation and/or the side friction development between the tires and pavement surface".

As a matter of conceptual convenience, centripetal force is equated to centrifugal force. Centrifugal force is a force that drivers feel pushing them outward. The term "centripetal acceleration" and its equivalent in horizontal curve design, "lateral acceleration," are used in AASHTO 2001 guidelines, as they are fundamentally correct (AASHTO 2001).

However, there is some disagreement on the exact definition of lateral acceleration. The majority of researchers and AASHTO (2001) guidelines consider it equivalent to the entire centripetal acceleration. On the hand, some researchers, such as Craus and Livneh (1978) and Bonneson (2001), have different explanations for it. In their studies, they named a portion of centripetal

acceleration as lateral acceleration. Bonneson (2001) explained "Lateral acceleration represents the portion of centripetal acceleration sustained by side friction". He represented the general relationship between these two accelerations as:

$$a_f = a_c - a_e \qquad (2.6)$$

where

a_f = acceleration sustained by friction or lateral acceleration ($a_f = gf_D$)(m/s^2)

f_D = coefficient of side friction demanded

a_c = centripetal acceleration ($a_c = v^2 / R$)

a_e = acceleration sustained by superelevation ($a_e = ge/100$)(m/s^2)

By combining the equations provided in the definition of each acceleration term a more common equation related to side friction demand, superelevaton rate, speed and radius of curve is:

$$f_D = (v^2 / gR) - e/100 \qquad (2.7)$$

where

v = vehicle speed (m/s),

R = radius of curve (m)

e = superelevation rate (percent)

The first group of researchers used another term to refer to this latter type of lateral acceleration. They called it unbalanced acceleration, which will be

explained later in the chapter. Lateral acceleration experienced by the drivers and the choice of speed on highway curves are the points of particular interest in highway geometric design. An explanation of car-driver behaviour may lie in the lateral acceleration because it is felt by the driver and passengers and at the same time affects the tire-pavement friction force. (Glennon et al. 1983).

Lateral acceleration is the result of the effect of different variables of curve driving. Researchers including Ritchie et al. (1968), Kneebone (1964), and Moyer and Berry (1940) measured the value of the lateral acceleration experienced by vehicle on curves. It was generally observed in these measurements that maximum lateral acceleration values tolerated by drivers decrease with increases in travel speed. This decrease in the value of lateral acceleration results from drivers being more careful when evaluating driving risk, which increases with increasing travel speed. It should be noted however that the lateral acceleration values themselves are not uniform in the various measurements. Nonetheless, the trend of these values when measured against travel speed is the same in almost all these studies (Craus and Livneh 1978).

In many cases, horizontal curves are circular curves, directly join tangent roadway sections at either end with no transition curve. Therefore, when a vehicle enters a curve, it theoretically encounters an instantaneous increase in lateral acceleration from a minimum level of the tangent section to the full lateral acceleration required to track the particular curve. The opposite occurs when the vehicle leaves a horizontal curve. In reality, a gradual change in lateral acceleration occurs rather than such instantaneous change, as drivers steer a

spiral or transition path as they enter or leave a horizontal curve. The design of the superelevation transition section can be used to partially offset the changes in lateral acceleration (Harwood and Mason 1994).

2.3.2 Speed and Lateral Acceleration

Ritchie et al. (1968) investigated the relationship between driving speed and lateral acceleration during normal curve driving. A total of 50 drivers were involved in their study. Each one drove on a 190-km segment of Ohio highways, which contained 227 identifiable curves. Each driver used the same unmodified 1962 Buick Invicta station wagon. The operating speed and lateral acceleration was recorded in the curves. The accelerometer was fastened to the floor of the car just below the driver's seat. The data were distributed into 10 speed ranges: below 30 km/h, above 95 km/h, and intervals of 8 km/h in between 30 km/h and 95 km/h. Within each speed group a mean and a standard deviation for lateral acceleration were computed for each driver.

The results showed a strong inverse relationship between speed and lateral acceleration for speeds above 30 km/h. The explanation of this relationship suggested some corollary hypotheses for future analysis (Ritchie et al. 1968).

- The primary criterion for the selection of speed in curves - below the posted legal speed limits - is the lateral force developed during driving.
- The kinesthetic perception of lateral force is the basic mode by which the driver obtains information for use in driving.

- There is an interaction between visual perception and kinesthetic perception, which develops quickly during the acquisition of driving skill, which may be degraded by drugs and changes due to age.
- Driver's observed decrement in lateral force as speed increases reflects the driver's estimate of increasing danger.

Studies have also shown that drivers adjust their speeds on curves so that maximum lateral accelerations tolerated by drivers decrease at high speeds. The study by Reymond et al. (2001) led to the formation of a new theoretical driver model that relates the choice of maximum driving speed on curves to perceived lateral accelerations. The new driving model predicts a pattern of a decrease of maximum lateral accelerations with speed and provides an explanation of the variations of this pattern attributable either to changes in driving style or to a modified perception occurring in a driving simulator.

Felipe and Navin (1998) in their study observed the driving behaviour of drivers on small radius curves of 16 and 26 m at the mean speed ranges from 30 km/h to 40 km/h. They also recorded the same information on curves of radius 90 and 120 m of two-lane undivided rural highway with driving speeds of 70 to 80 km/h. They concluded "that the speeds selected by the drivers were higher when the small curves were driven counter-clockwise (i.e. left-turn curve) rather than clockwise (i.e. right-right curve)". The study of Felipe and Navin (1998) was focusing on relationship between speeds and radius of curves and was not explaining the reason why the speed is higher in case of left-turn curves.

2.4 Unbalanced Lateral Acceleration and Point Mass Model

If we reproduce the point mass equation (refer to Equation 2.1), the superelevation value offsets a portion of the lateral acceleration on a superelevated curve, such that:

$$a_{net} = (V^2/127R) - e/100 \qquad (2.8)$$

where

a_{net} = unbalanced lateral acceleration in g's

e = superelevation rate (percent)

V = speed of vehicle (km/h)

R = radius of curve (m)

The unbalanced portion of lateral acceleration of the vehicle may be defined as the measure of the forces acting on the vehicle that tend to make it skid off the road. The vehicle's tendency to skid must be resisted by friction between tire and pavement. The vehicle will skid off the road unless the tire/pavement friction coefficient exceeds the side friction demand. The assumed value of lateral acceleration – side friction factor f - is based on the tolerable limits of occupants of the vehicle and is far below the threshold of tipping or sliding out of a typical passenger car (Carlson and Mason 1999). Bonneson (1999) and Harwood and Mason (1994) named a_{net} as the side friction demand factor (f_D), which has already been shown in Equation 2.7.

Previous researchers have concluded that vehicles during entry and exit from a horizontal curve shift laterally in the traffic lane. In addition, other research

indicates that most drivers momentarily adopt a path radius that is sharper than that of the roadway curve. Bonneson (2000) concluded that lane shift by drivers as they enter the curves is due to the unbalanced lateral acceleration that act on the vehicles as they enter the curve.

2.5 Side Friction

Side friction has been referred to as lateral ratio, unbalanced centrifugal ratio, cornering ratio, unbalanced lateral acceleration, and unbalanced side friction depending upon the researcher and country or institute performing the study (Merritt 1988). Emmerson (1969) worked with the relationship between car speeds on curves and side friction factors. He concluded that almost 80 percent of the vehicles experienced a friction factor of less than 0.15 on curves with radii of between 351 m and 196 m. Sites with very small radii, 10 m and 21 m, had mean factors of 0.22 and 0.27, respectively. McLean (1983) claimed that the side friction factor is an outcome of driver behaviour not explanation for it.

Tests conducted in 1936 showed that the average side friction factor of 0.16 is related to a driver's point of discomfort. In a ball-bank indicator, a reading of 10 degrees represents a close fit to this average side friction value based on drivers "side pitch" (drivers feel leaning or tilting of their body at one side). This value was a primary factor or benchmark for future research in ball-bank indicator for curve design. The same report maintained that higher side friction values could be tolerated for lower speeds due to less severe consequences if a driving error was committed (Merritt 1988).

Morrall and Talarico (1994) concluded that regardless of the type of vehicle, most drivers experience the same level of comfort on horizontal curves because safe side friction factor values appear to be relatively constant across the vehicle types investigated.

The values of side friction from various studies have been used in developing the horizontal curve design criteria in the various AASHTO guidelines of geometric design of highways. The upper value is used for low-speed urban designs and represents an increased sense of tolerance or more discomfort to the driver in urban conditions. The lower values indicate a lower degree of driver discomfort when compared with the urban driving situation. These side friction values have not been correlated with ball-bank indicator readings (Merritt 1988).

2.5.1 Theoretical Side Friction versus Observed Side Friction

Lamm et al. (1991) in their study also compared the side friction demand versus side friction assumed on the basis of geometric design, operating speed, and accident data (refer Table 2.1). A comparative analysis of side friction demand versus side friction assumed was carried out with respect to degree of curve as the independent variable. It was concluded that:

1. Side friction increases as the degree of curve increases.
2. Theoretical side friction is higher than the observed side friction on curves up to 6.5 degrees.
3. In case of curves greater than 6.5 degrees, observed side friction is higher than the theoretical side friction.

4. The gap between theoretical and observed side friction increases with increase in degree of curve.

In the case of operating speed as the independent variable, it was concluded:

1. Theoretical side friction is lower than observed side friction up to operating speeds of 80 km/h.
2. In case of operating speeds greater than 80 km/h, theoretical side friction is higher than observed side friction.
3. The gap between theoretical and observed side frictions increases with decrease in operating speeds.

2.5.2 Side Friction and Factor of Safety

Researchers have expressed several concerns in the literature regarding AASHTO's guidelines for horizontal curve design. Specifically, the maximum design limits of side friction factors recommended by the AASHTO Green Book are considered to be too conservative. The first concern related to these limits is that they are based on the studies conducted from 1920 to 1952 and today's drivers have potentially become more tolerant of lateral acceleration due to changes in attitude and vehicle cornering capabilities. The second issue raised is regarding the relationship between the design speed and side friction. Differing opinions are held by various agencies about the level of side friction suitable for a given speed, especially lower speed. (Bonneson 2001).

The side friction factors that are currently used in the high-speed and low speed design procedures were obtained by using vehicle occupant comfort as the selection criteria. These criteria assume that drivers limit their speed on

curves to ensure comfort for the occupants of the vehicles and discomfort that driver feels is directly related to the unbalanced side friction. Several concerns accompany this assumption. For instance, the speed at which discomfort (side pitch) first becomes noticeable may be slower than necessary for safety, and the level of discomfort felt by a driver may not be solely related to side friction only. These assumptions do not consider vehicle characteristics or constant safety factors over the range of design speeds (Fitzpatrick 1994).

The speed on a curve, at which the driver observes discomfort owing to the centrifugal force, can be accepted as a design control for the maximum allowable amount of side friction (Morrall and Talarico 1994). AASHTO guidelines also provide a warning that other factors such as swerving and increased steering effort are required to control a driver's speed at conditions of high friction demand. AASHSTO guidelines state that "the maximum selected side friction factors should be conservative for dry pavements and provide a margin of safety for operating on pavements that are wet as well as ice or snow covered".

Rather than conducting road tests many researchers used assumed values of side friction to calculate the margin of safety a vehicle has when cornering (Morrall and Talarico 1994). However, some researchers including Salt (1976) calculated the margin of safety through field test. He used skid trailers connected to a tow vehicle in a way that the longitudinal axis of the trailer is at an angle to the line of motion of the two vehicles. As the tow vehicle moves, the trailer also moves forward with the wheels rolling forward, with a side skid motion. Due to lack of a driving force on the trailer tires, combined with the absence of the

vehicle roll that occurs during cornering, skid trailers do not provide a realistic model of a side skidding vehicle. Lamm et al. (1991) used the point-mass equation to calculate the amount of side friction demanded. Relationship between curve geometry and friction factor were then established. They found that drivers demand more friction on curves shaper than 2 degree/100 m and at speeds lower than 80 km/h. By observing driver behaviour on curves, McLean (1974) also found that drivers tend to demand more side friction on tighter, highly superelevated curves. Most researchers in this area insist that instead of using the tire's available full friction for cornering for design, friction factors should also provide the braking friction and should ensure that enough friction remains for other manoeuvres. As the side friction factors are the same as unbalanced lateral accelerations, measured in g's, in the plane of the road, one can use an accelerometer to measure the side friction factor directly (Morrall and Talarico 1994).

2.5.3 Side Friction and Ball-Bank Indicator Reading

The ball-bank indicator readings of 14-degrees for lower speeds to 10-degrees for the higher speeds are generally accepted. These readings reflect the similar tolerable driver discomfort behavior explained by "side pitch outward". Many tests conducted earlier also concluded that a side friction factor of 0.21 for speeds below 32 km/h and of 0.18 for speeds of 40 to 48 km/h were considered to be acceptable to ball-bank readings of 14-degrees and 12-degrees respectively (Merritt 1988).

Morrall and Talarico (1994) in their study worked with the relationship between side friction and ball-bank indicator readings. They used the regression analysis to find out the relationship between them. They found that coefficients of determination between side friction factor and ball-bank angle for the highway sites range from 0.976 to 0.645. The correlation coefficient between ball bank angle and side friction factor is lower for flatter curves than for sharper curves. Based on the 1990 version of AASHTO design criteria for horizontal curves, curves flatter than 1000 meter provide a very high margin of safety. For the sharper curves, speeds more than 90 km/h can be achieved before driver discomfort is noticed. This illustrated that the provided margin of safety on these curves by design guidelines of AASHSTO are lower than those provided on the flatter curves (Morrall and Talarico 1994).

2.6 Body Roll and Rollover

Motor vehicle rollovers have always been a source of concern, because of a relatively high risk of occupant death or injury as compared with other types of crashes. In year 1999, more than 10,000 people were killed in light-vehicle rollovers, almost a quarter of over 40,000 traffic crash victims in the United States for that year. During the period 1995–1999, 7 percent of light-vehicle tow-away crashes involved rollover, but these crashes accounted for 31 percent of light-vehicle occupant fatalities. The chances of death or injury are especially high for single-vehicle rollovers, which represent approximately 80 percent of light-vehicle rollover crashes (NHTSA 2002). The Insurance Institute for Highway Safety (2000) has provided that "single-vehicle crashes involving rollover

accounted for 43 occupant deaths per million registered passenger vehicles in 1999". This data shows the importance of measures to be taken to reduce the light-vehicle rollovers specially those involving single vehicles.

Body rollover is the condition that occurs, when the vehicle turns on one side 90 degrees or more about its longitudinal axis in such a way that it makes contact with the ground (Gillespie 1992). Just like anything in a circular motion when any vehicle rolls, it must have a central point about which it rotates or rolls. In a car this is known as the roll centre, which can be considered pivotal point around which body roll occurs.

Lateral acceleration, braking and longitudinal acceleration all put a tremendous strain on the car. Frames, bodies and other seemingly indestructible parts twist and bend. The effect of centrifugal force during cornering applies on the total car mass through its centre of gravity. This force is experienced as "lean" or "sway," but most commonly known in auto racing and vehicle dynamics as "roll". The effect of this centrifugal force on the centre of gravity is totally dependent on speed; the higher the centre of gravity, the lower the speed at which a car will reach its maximum roll (AutoZine 2003).

2.7 Operating Speed

Operating speed is the speed selected by drivers under free-flow-conditions and is generally the 85th percentile speed. This is the speed that 85-percent of drivers will not exceed. McLean (1983) found that there is no empirical evidence that drivers respond to actual or subjective predicted side friction in selecting

their speed around curve. McLean claims that it is better to view friction demand as an outcome of speed behaviour, rather than determinant of it. Harwood and Mason (1994) in their study evaluated the AASHTO's (1990) geometric design policy for safety and criticized it for providing unknown levels of safety. A speed survey conducted by the British Columbia Ministry of Transportation and Highway in 1994 found an 85th percentile speed of 80 km/h in a section of posted speed of 60 km/h. This attitude of high speeding raised the question about the current design procedures. Assuming that drivers adopt speeds that provide them with a comfortable ride, current highway design practice based on experiments conducted in 1930's may not fully accommodate the geometry of highway elements with modern vehicles and driver performances, and therefore may not provide adequate safety (Felipe and Navin1998).

A very visible indicator of inconsistency in alignment design is the change in the speed. A change in the mental workload of drivers due to inconsistency is not observed so readily although it may lead to more accidents due to drivers inadequately coping with the increased workload (Nicholson 1998). The design speed concept has been the basis of the majority of the geometric designs. The design speed concept is based on two fundamental principles (Krammes et al. 1995):

1. The design speed should be representative of the uniform speed at which majority of drivers desire to operate.
2. Within a section of road, all curves should be designed for the same speed.

2.8 Selecting Advisory Speeds and Ball-Bank Indicator

There is no adequate and universally accepted criterion for determining advisory speed, which results in non-uniform and too low-posted speeds in most cases. As a result, posted speed may end up of little significance for drivers. Unfamiliar motorists who find it safe to drive over the advisory speed will place themselves in a potentially hazardous situation when encountering the occasional curve posted with a realistic and meaningful advisory speed. Therefore, non-compliances of posted speed have become a potential safety threat and have caused accidents on curves. Two methods are being used to set the advisory speed for the curves, i.e. ball-bank indicator and standard curve formula. The criteria used in these methods for setting the advisory speed have not changed since 1930's (Chowdhury et al. 1991).

The ball-bank indicator is the main tool for setting advisory speed on horizontal curves and has been in use for quite some time. A poll conducted by David R. Merritt in 1987-88 of all 50 states of the U.S, displayed that a 10 degree reading at 55 km/h was still accepted as "sacred" generally (Merritt 1988). In a survey conducted in 1994, 88 percent of states, cities, and counties that responded indicated that they use the ball-bank indicator to set the safe speeds (Fitzpatrick et al. 1995). However it is a matter of great concern that researchers and agencies do not agree on common readings of ball-bank indicator for setting the advisory speeds. Therefore, different agencies and researchers have different recommendations of speed limits on the basis of the same readings of ball-bank indictor, as shown in below given Table 2.2.

Table 2.2:Speed (km/h) Suggestions for Different Values of Ball-Bank Indicator by Different Authorities/Researchers

Agency/ Researcher	9 Degree	10 Degree	12 Degree	14 Degree	16 Degree	20 Degree
Moyer et al. (1940)	-	≤80	<48	<32	-	-
FHWA (1983)	-	56	32-56	32	-	-
David (1988)	-	56-80	-	<32	-	-
Chowdhury et al. (1991)	-	-	>64	-	48-64	<48
AASHTO (1994)	-	>48	32-48	<32	-	-
Carlson (1999)	>50	-	30-50	-	<30	-
AASHTO (2001)		55-80	40-50	30		

The second method used to determine the advisory speed is use of nomograph discussed in the Traffic Control Devices Handbook (TCDH). This handbook uses the standard point mass formula shown in Equation 2.1.

The nomograph assumes a friction factor of 0.16, which corresponds to the speed at which discomfort begins for an average rider in a 1930 vintage car. A study conducted by Chowdhury et al. (1991) revealed that the average friction used by the 50^{th} percentile driver was 0.22 and was 0.29 for the 85^{th} percentile

driver. These values are nearly twice the current value being used in establishing advisory curve speeds. Drivers accept higher side friction on lower speed curves rather than what is currently assumed for road design, where the friction values used by drivers are at least 50 percent greater than those assumed in road design. In comparison, cars on dry pavements can generate side friction values ranging from 0.65 to 0.90 before skidding out (Merritt 1988). Therefore, the side friction used on curves depends more on driver comfort rather than by the limits of the vehicle-pavement interaction (Chowdhury et al. 1998).

2.9 Conclusion

On the basis of literature review presented in this chapter it is quite obvious that lateral acceleration is an important feature of curve driving. It relates to almost every element of curve driving and is felt by both the driver and passengers alike. It is also obvious that only a few studies are providing the relationship between lateral acceleration and these features. Particularly no significant attempt has been done to evaluate the effect of different features of vehicle on observed values of lateral acceleration. The review also shows that previous work does not provide the answer of the question why operating speeds of vehicles are higher in case of left-turn curves than for right-turn curves for small radii curves. There is also a need to investigate whether this pattern of different speeds on different directions will be continued in case of medium and large radii curves and the causes for that. There is also a need to update the parameters of curve driving to meet with modern car and geometric design parameters

Another area where further study is required is determining the relationship between observed lateral acceleration and theoretical lateral acceleration. In this regard there is a need to find out the effect of the values of observed to the theoretical lateral acceleration in the below given areas. Furthermore, there is need of development of models for these relationships:

- Peak values of lateral acceleration.
- Average value of lateral acceleration
- Peak value in case of uneven weight
- Average value in case of uneven weight

There is also need to figure out the effect of the above values of lateral acceleration on the safety against skidding.

Chapter 3
Data Collection

This chapter provides details on how the database for this study was developed. In the subsequent chapters, the same data were used to analyse the relationships between some features of curve driving and to develop the model of this relationship. Section 3.1 introduces the data, their sources and the criteria adopted for site selection. Section 3.2 presents complete details of the equipment used in this research and its functions. Section 3.3 goes through the process adopted and arrangements made for data collection. Finally, Section 3.4 explains the way the raw data of lateral acceleration were downloaded and saved.

3.1 Site Selection

Curve geometry data were extracted from the as-built construction plans of seven two-lane rural highways located in eastern Ontario. These plans were collected from two major sources:

- The Planning and Design Office of the Eastern Region of the Ontario Ministry of Transportation (MTO) provided data for the King's Highways.
- The Roads Department of the United Counties of Stormont Dundas and Glengary (SDG) supplied the data for the Secondary Highways and County Roads.

The provided as-built plans were very carefully scrutinized for selecting appropriate segments of roads, which could represent a variety of highway classifications, terrains and design/advisory speeds. Initially 120 curves on these

seven two-lane rural highways were available for this study. The combined length of all segments, where these curves were located, was 150 km. These curves were further investigated through site visits. Finally, selection criteria were developed for site selection. After this second phase of investigation, the number of curves was reduced to 71. The criteria developed for selection were:

- No signalized or major intersection to enable maintaining a constant speed during the data collection.
- Not in built-up areas or inside town to avoid interruption.
- No recent improvements so that the data collected in this study can complement other studies carried out on the same area.
- No other adjacent physical features that may create unusual operating or hazardous conditions.

At the time of data collection, some decisions were taken due to construction activities on Highways 17 and 41, as well as slow-moving vehicles, and other activities on Highway 12. In the light of these factors, actual curves included in this study were reduced to 60. All these details have been summarized in the tables attached as Appendix A at the end of this thesis. The radii of these selected curves ranged from 300 to 1200 m, while the curve length including spirals ranged from 100 to 1000 m. The general characteristics of the highway segments used in this study are summarized in Table 3.1:

Table 3.1: Summary of Study Highways and Curves

Highway Number	Highway Type	Design Classification	Segment Length (km)	Initial Number of Curves	Final Number of Curves	Posted Speed (km/h)
31	Secondary Highway	Not Provided	25	14	10	80
15	King's Highway	RAU 100	24	24	10	80
7	King's Highway	Not Provided	12	12	10	80
17	King's Highway	RAU 100	25	10	7	90
43	Secondary Highway	Not Available	18	7	7	80
12	County Road	Not Provided	18	18	5	80
41	King's Highway	RCU 80	28	35	11	80
Total			150	120	60	

An important geometric element, (superelevation rates) was not available in the provided details. Therefore, arrangements were made for measuring the superelevation at all selected curves by using a digital ball-bank indicator powered by a detachable battery. Superelevation rates of the curves were measured at three points near the centre of each curve and in each direction. These six readings of both directions were used to calculate a single average reading of superelevation rates of each curve. This exercise was conducted because with the course of time, settlements and deformations of pavement could affect the uniformity of the surface. Superelevation rates measured ranged from 0.032 to 0.069 (1.81 to 3.93°).

3.2 Data Collection Equipment

Selection of the equipment used in the data collection is an important element of any field-based study. Two types of equipment were used at the same time for collecting the lateral acceleration simultaneously. The test vehicle, computer and other electronic items used in this study were of latest version and models and representative of the prevailing conditions.

3.2.1 Ball Bank Indicator

Airplanes first used the ball-bank indicator so that pilots could judge tilt of the wings in relation to horizon. In 1937, the Missouri State Highway Department first used the ball-bank indicator for measuring the centrifugal force on curves (Merritt 1988). Following this, the ball-bank indicator became the main tool being used to set advisory speed on horizontal curves. As mentioned earlier, a recent survey showed that 88 percent of states, cities, and counties that responded use the ball-bank indicator to set the safe speeds (Fitzpatrick et. al. 1995).

3.2.2 Manual Ball-Bank Indicator

The manual ball-bank indicator is a simple instrument, which consists of a steel ball, sealed in a liquid filled curved glass tube. This glass tube is graduated from centre zero point outward to end of tube in degree of full circle and is free to roll laterally under the influence of the forces acting upon it (refer to Figure 3.1). It is important to make sure that following points are being followed during data collection (Merritt 1988);

1. Ball is in zero position when vehicle is horizontal.

2. Tire pressures are all equal.
3. Vehicle is driven all around the curve at constant speed and parallel to the centre lane of the curve.
4. There is no cutting corner during driving

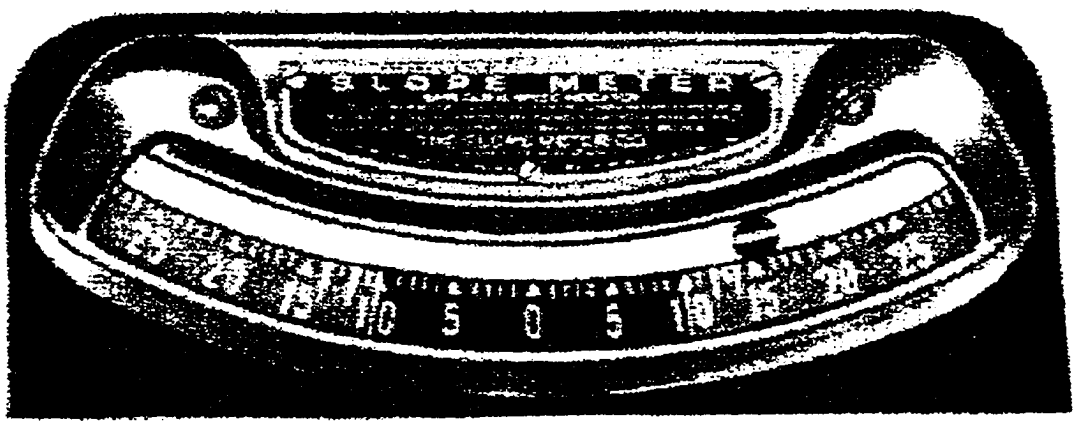

Figure 3.1: Ball-Bank Indicator

3.2.3 Fundamentals of Ball-Bank Indicator

Ball-bank indicator's readings are the measure of centrifugal forces on the vehicle and driver in the vehicle. When a vehicle passes through a curve, the effect of centrifugal force on the vehicle will cause the ball to roll out like a pendulum. For superelevated curves, the weight of the vehicle opposes the centrifugal force. If the vehicle speed is same as the equilibrium speed for the curve condition the resultant force will be perpendicular to the pavement surface, and if there is no vehicular body roll, the ball will read zero degrees. If the speed is more than the equilibrium speed, side friction forces acting inward will react on the vehicle and if body roll is not considered in this case again then the value of

ball-bank indicator will represent a direct function relationship with side friction (Merritt 1988).

Carlson and Mason (1999) explained the relationship between different forces affecting ball bank indicator reading as: "the ball bank reading (α) at any time equals the combined effect of the lateral acceleration (centrifugal force) angle (θ), the superelevation angle (ϕ), and the body-roll angle (ρ)" (refer to Figure 3.2).

$$\alpha = \theta - \phi + \rho \qquad (3.1)$$

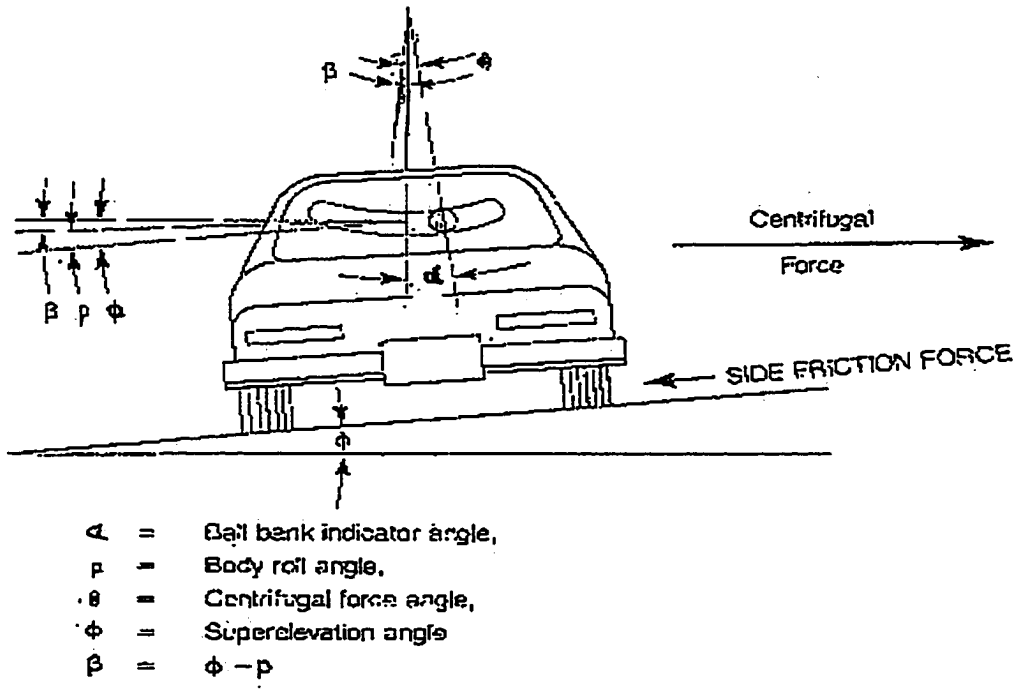

Figure 3.2: Geometry for Ball-Bank Indicator (Merritt 1988)

As explained earlier, on a superlevated curve, the superelevation offsets a portion of the lateral acceleration, such that:

$$a_{net} = (V^2/127R) - e/100 \qquad (3.2)$$

where

a_{net} = unbalanced lateral acceleration in g's (9.807 m/s^2)

e = superelevation in percent (m/m)

V = speed (km/h)

R = radius of curve (m)

The unbalanced portion of lateral acceleration of the vehicle is a measure of the forces acting on the vehicle that tends to make it skid off the road. To determine the significance of the components that make up the ball bank indicator reading, the unbalanced lateral acceleration can be separated into two components: lateral acceleration and superelevation, which has already been explained in Equation 3.2 (Carlson and Mason 1999).

3.2.4 Electronic (Digital) Ball-Bank Indicator

A contemporary digital ball-bank indicator is also available in the market, and was used in this study. Arrangement was made to make it attachable at one side with a 12-volt battery to determine the superelevation rates as explained earlier (refer to Figure 3.3a). Originally it can be connected to vehicle's cigarette lighter or any other power source that can supply a 12-volt D.C current. The digital ball-bank indicator used in this study was Rieker's RDI digital display model RDS7-

BB-C, manufactured by Rieker Electronics Inc., USA. This instrument has the following features:

- $\pm 25^0$ input range.
- Auto levelling (no need for a perfectly level mounting surface).
- Velcro-mounting for quick installation and easy removal.
- Angle display in degrees, percent grade, or inch per foot rise.
- 0.1^0or 0.01^0 display resolution.
- Relative zero (regardless of road level data collection will start from 0°).
- Min/Max reading (freezes the highest left and right corner readings).
- $\pm 10^0$ audible alarm.
- RS232 serial output (PC compatible).

The RDS7-BB-C is powered by a standard 12-volt cigarette lighter style cable connection with a RS232 serial port connector (refer to Figure 3.3b). The RDS7-BB-C can be mounted on any surface that is within 10 degrees of level. Placing the unit in the desired location can determine appropriate surface level. If the unit displays less than 10 degrees then the chosen location is fine. With the vehicle on a relatively level surface, power up the unit and look at the digital display to determine if the unit is reading 0 degrees or level. If the selected mounting location is level, the unit is ready to begin operation.

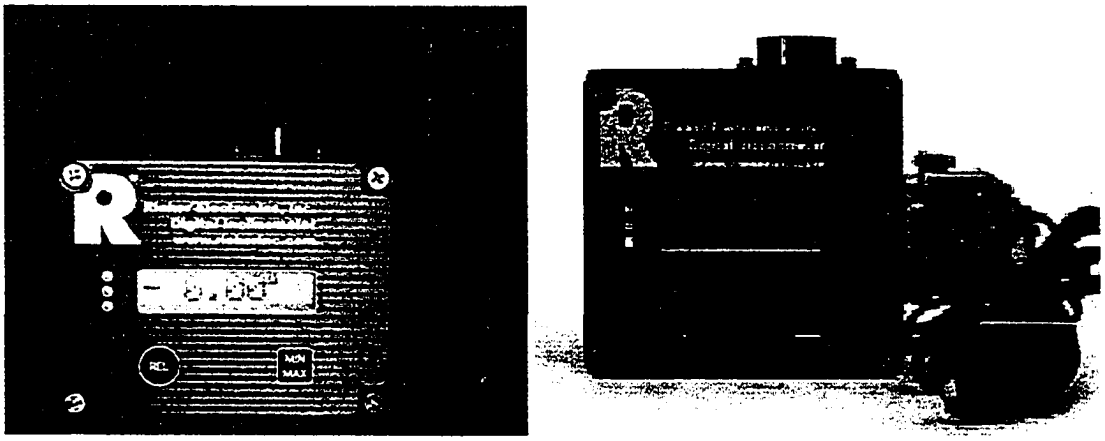

(a) With Detachable Battery **(b) With RS232 Serial Output**

Figure 3.3: Digital Ball-Bank Indicator

If the unit is not level, but within ± 10 degrees, the REL button should be pressed and released. The display will read "REL ON" for one second then revert to normal with the unit reading zero. If after pressing the REL button display reads "OVER REANGE" the unit is not within ± 10 degrees from level. This unit must be re-positioned and auto levelling procedure repeated.

Once the RDS7-BB-C unit has been auto levelled it is ready to conduct measurements. Before driving the stretch of road with the curve that will be evaluated, press the MIN/MAX button slowly three (3) times: the first press will display "LEFT" for one second, then freeze the (-) side reading. The second press will display "RIGHT" for one second, then freeze the (+) side reading. The third press of the MIN/MAX button will display "RESET", then immediately go back to normal function. When in the act of determining safe curve speed, the MINIMUM reading corresponds to left hand turns and the MAXIMUM corresponds to right hand turns. The RDS7-BB-C unit comes factory set to sound an alarm at ± 10 degrees, allowing the operator to safely drive through the corner

and keep eyes on the road, not the unit. If the system determines that the vehicle has exceeded ± degrees, it will sound an alarm, which indicates to the operator to press the MIN/MAX button to display the highest value achieved. This will provide the necessary information to determine the safe speed for that curve.

A laptop computer can be used to record the RS232 output in conjunction with the RDS7-BB-C by plugging in the appropriate Rieker Power Cord. This modified power cord splits to provide a serial port connector as well as the cigarette lighter adapter. Installation is done by first, inserting the cable's single-end parallel connector into the RDS7-BB-C's parallel port then attaching the computer serial port connector to the laptop's serial port. If no serial port in the laptop is available it can be attached by using USB adapter, which can be connected to laptop through USB cord and can provide more than one connection to laptop. This type of USB to RS-232 adapter Model QSA-100 is manufactured by Quatech Inc., and was also used in this study (refer to Figure 3.4). Finally, by inserting the cigarette lighter adapter end of the cord into the cigarette lighter socket of the vehicle –the unit and computer can be switched on.

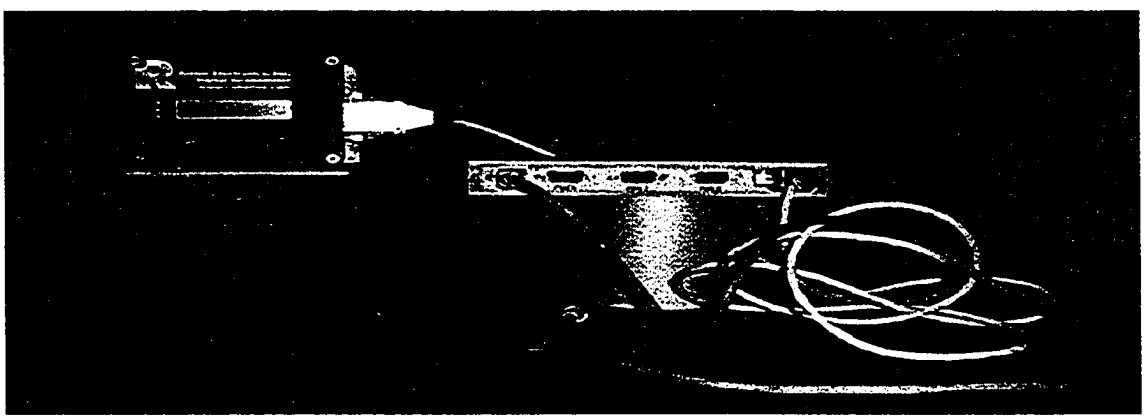

Figure 3.4: Ball-Bank Indicator and Quatech QSA-100 USB- RS to 232 Adapter

When power is supplied to the unit, data will begin to flow to the laptop. A single column of numbers will appear on the screen with a "+" or "-" sign to distinguish between a right or left turn. Pressing the MIN/MAX button will stop the flow of data from the RDS7-BB-C. For continuous recording of values in each run, it can be connected to the Microsoft Hyper Terminal from where values could be saved in any desirable software for further analysis.

3.2.5 Electronic Accelerometer or G-Analyst

To determine lateral acceleration on horizontal curves and ramps, an electronic accelerometer can provide an alternative to the ball-bank indicator. These types of accelerometers are also used in race cars to record performance of different features of car driving such as acceleration, speed, and brake and steering. An accelerometer is a gravity sensitive electronic device that can measure the lateral acceleration that drivers experience while the vehicle is travelling through horizontal curves.

3.2.6 Corsa Electronic Accelerometer

The Corsa Electronic Accelerometer, manufactured by Corsa Instruments Inc. was also used in this study to determine the lateral acceleration. The hardware accompanying the Corsa instruments data acquisition package includes the following:

- Data acquisition box (DAB) or data logger/sensor box, equipped with 512k RAM and three built-in accelerometers (refer Figure 3.5).
- Driver control box (DCB) (refer Figure 3.7)

- Driver control box cable (14/15 pin) (refer Figure 3.7)
- Serial cables (9 pin to 9 pin) (refer Figure 3.5)
- RPM interface box (refer Figure 3.6)
- Additional sensors (refer Figure 3.6)

The Corsa instruments data acquisition system comes complete with software for Microsoft Windows to perform the following work:

- Configure the data acquisition box to record data within preset parameters.
- Communicate between the data acquisition box and the PC.
- Send configuration files to the data acquisition box, and retrieve stored or real-time data from the data acquisition box.
- Display, manipulate, and print the recorded data.
- Export the recorded or manipulated data to lotus 1-2-3, Microsoft Excel or other database programs, which use a comma-delimited format.

The data acquisition box is used to record and store the data supplied to the equipment. Its storing capacity (memory) varies with cost. Every time data acquisition box approaches the memory storage limits, it will notify the user. It has three built-in sensors and five additional sensors. In addition to lateral acceleration, it can record longitudinal acceleration and box temperature as a built-in function. Furthermore it has provisions for recording throttle, steering, brake, engine RPM, and speed through additional sensors.

The driver control box is the main control panel. It has an on/off button to start or quit the work and stop/run button to start or stop the recording of data. It

has light indicators such as power and status lights to indicate the stage of data collection of that time. It has one additional button used to mark the reading of any particular spot. After recording the data it can be saved in WINCORSA Software for further processing.

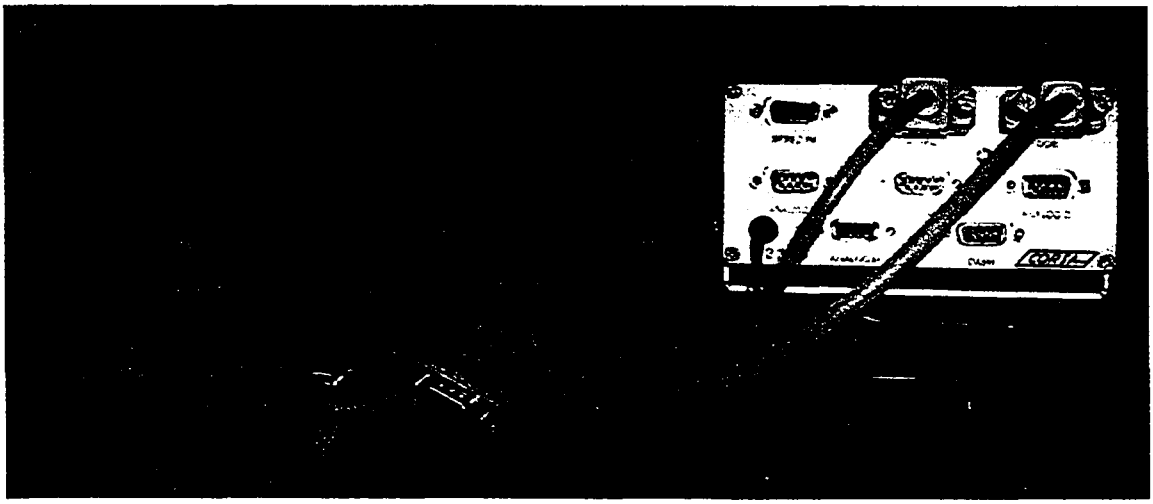

Figure 3.5: Corsa Data Acquisition Box with Serial and DCB Cables.

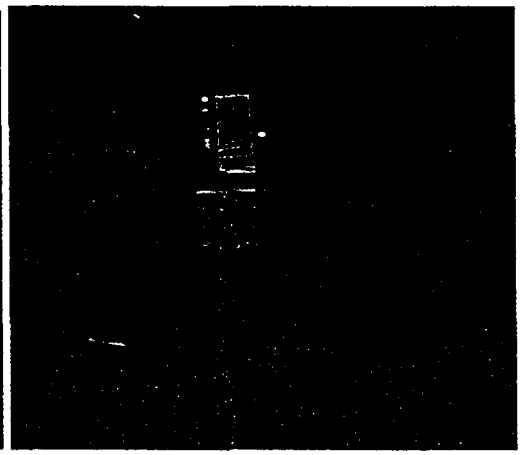

Figure 3.6: Sensor with RPM Cable Figure 3.7: Driver Control Box (DCB)

The data acquisition box (DAB) should be mounted at a level place, and perpendicular to the car floor. It does not matter which side (front or back) the

connectors face, but the box should not be mounted at an angle position to the car floor. The box has four threat inserts to mount at the required place. These are closed from the inside, and can be used as a bolt. Accelerometer data are affected by the mounting angle. Small errors can be corrected in software, but if the mounting angles are large, the results may not be accurate. Theoretically, the best location for the box is at the centre of gravity of the car. This is often not possible in the real world. The following are common locations:

- In formula cars, behind the drivers seat, or under the driver's knees, or anywhere it fits.
- In most other cars, on the floor, in front of or behind the driver's seat, or on the passenger side.
- On the top of the transmission tunnel.

The box draws less than ½ amp power, and has a built-in power filter and a fuse. The power connector supplied with the system is the standard type commonly used for trailer connections. Generally, the best solution is to connect the red wire directly to the position terminal of the battery. The black wire should be connected to a solid chassis ground or the negative terminal of the battery.

It is important to choose a location for the driver control box (DCB), which is safe and convenient for the driver and crew. The supplied 15-pin cable can be used to attach the DAB terminal, labelled 'DCB' to the Driver Control Box. The serial interface cable supplied with the system is used to connect to the computer. Pushing down on the toggle switch at the end of the DCB will turn the power light on, and will release the spring-loaded toggle switch. If the input power

to the Corsa box is fine, the power light will be green. If the power light is orange or red, the box is not receiving power from the car and is running on its internal batteries. Each time the box is turned on, it does a quick self-test and normally goes directly into "run" or "stop" mode depending on how the switch is set. If the status light is red or blinking, the self-test has failed, indicating something is wrong with the box. When this switch on the DCB is flipped to the "run" position, the box will record data following the instructions in the current configuration file. The run light will be flashing green. When box memory is 90% full, the light will turn orange. When the memory is completely full, the light will turn red, and the box will stop recording data.

The stop/run switch must be in the "stop" position for the box to communicate with the PC. To send the data stored in the box to the PC, the serial cable must be connected and the box should be "on" and in the "stop" mode. From the PC menu, select "box" and "get data" and the data will start downloading. A legal MS-DOS file name should be allocated with the menu selection.

3.2.7 Test Vehicle

Data for this study were collected using a 2002 Toyota Corolla, Model CE. This test vehicle is currently one of the best-selling passenger cars and reasonably represents the fleet of passenger cars in this area (Toyota 2004). Toyota is a front-wheel-drive car having independent suspension (MacPherson Strut) with front and rear stabilizer bars. It has 1.8-litre four-cylinder engine. Other features include:

- Tread (track) width at front is 1.461 m and at rear side 1.451 m.
- Total length (L) is 2.464 m (wheels centre to centre distance)
- Overall length is 4.421 m
- Overall width is 1.695 m
- Overall height (H) is 1.385 m
- Minimum ground clearance is 0.119 m
- Co-efficient of drag is 0.31
- Curb weight 1176 kg. (2690 lbs.)
- Torque @ 4000 rpm is 187 kg. m
- Tire size and number: P175/65 R14 815

3.3 Data Collection Procedure

The following section explains the methodology used to collect the data in the field. It also includes the manufacturing of the frame -for holding the DCB- in Carleton University's workshop and power-supplied devices purchased from the local market to facilitate the task of data collection. This section also gives the details of seating arrangement inside the car at the time data was collected.

3.3.1 Driving Speeds

Speed limit was 80 km/h for all seven highways except Highway 17, which has a maximum speed limit of 90 km/h. Three driving speeds were selected for this study. Criteria for this selection were on the basis of a previous study on the same curves (Peyman 2003). In that study, it was found that average operating speed of passenger cars on these curves is 99.11 km/h in case of posted speed

80 km/h. The preliminary driving speed selected was the posted speed, and the second and third speed was around the operating speed. A middle speed was also added producing 10 km/h increment between all three speeds. This translated to speeds of 80, 90 and 100 km/h for the posted speed of 80 km/h and 90, 100 and 110 km/h for the speed of 90 km/h.

3.3.2 Data Collection Arrangements

Arrangements were made with the help of Carleton University Civil Engineering laboratory technicians to install the Corsa acquisition box on the backside rail of the front passenger seat through a frame made of clamps and aluminium section (refer to Figure 3.8). This setting was removable after each workday.

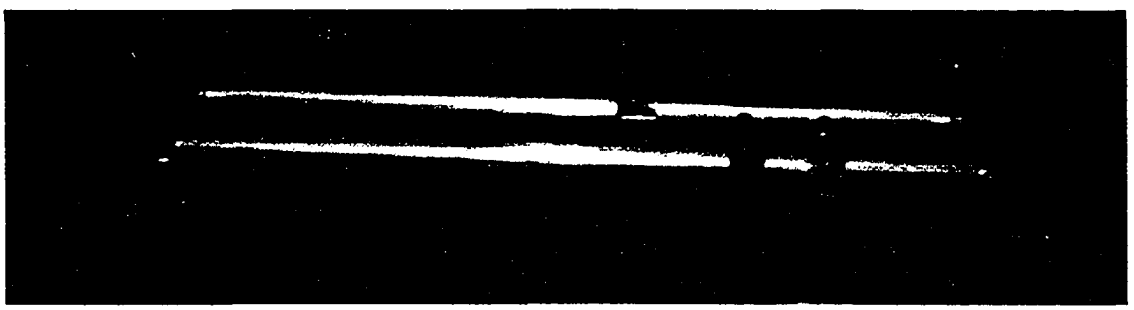

Figure 3.8: Aluminium Frame for Holding the Data Acquisition Box

Power to this instrument was provided through the car cigarette lighter. Frequency of data recording for this study was set to 10 readings per second. The Corsa acquisition box was attached to a laptop, and after every run the collected data were uploaded to the computer through the Corsa software. A unique file number was assigned to each set of readings to distinguish it from

other readings. For instance, in case of a northbound driving speed of 90 km/h on curve number 10 of Highway 31, the file number allotted was 31C10N90.

The ball-bank indicator was placed in the space between driver and front passenger seat. A wooden hollow box with velcro strips around it was manufactured to hold the ball-bank indicator in position (refer to Figure 3.9). The ball-bank indicator was attached to a laptop during driving. At the start of each curve, the box was sending the lateral acceleration data every 0.25-second by simply pressing the start button. These data were transmitted to the laptop's hard drive through Microsoft Hyper Terminal, and were saved in Microsoft Excel format at the end of each segment.

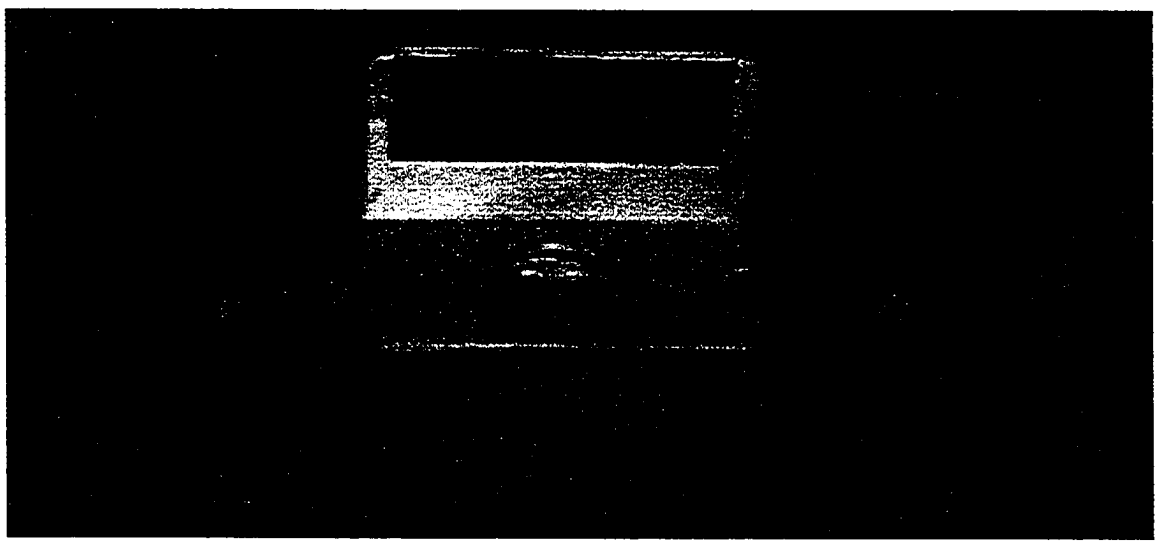

Figure 3.9: Stand for Ball-Bank Indicator with Velcro Mounting

At this point, there were three different instruments using the car's single cigarette lighter: the ball-bank indicator, Corsa accelerometer and laptop. The first two instruments required 12-volt power while the third needed 15-volt power. To overcome this problem, the car's cigarette lighter port was connected to a 12

volt triple socket adapter (refer to Figure 3.10). Two sockets were used to provide a connection to the ball-bank indicator and Corsa accelerometer while the third one was attached to a 175 watts converter to convert the 12 volt DC power to 115 volts AC power (refer to Figure 3.11). At the other end, the inverter was attached to the laptop adaptor to convert the 115 volts to the 15 volt AC power.

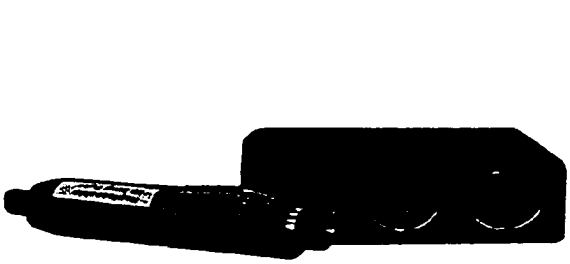

Figure 3.10: Triple Socket Adapters

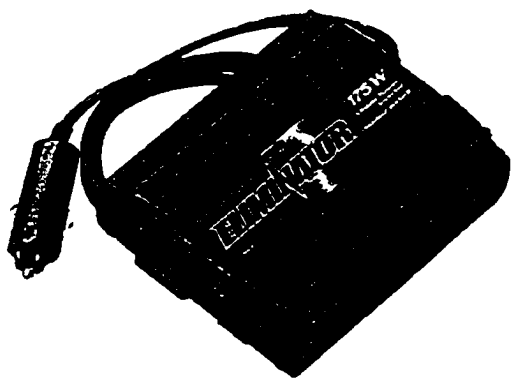

Figure 3.11: Inverter

Data were collected during weekdays and in daytime between 10:00 am to 6:00 pm. Before each run, the test vehicle would park on a level surface and the ball-bank indicator offset readings were recorded. Same offset readings were added in the ball bank indicator's collected values at the end of each day of work.

In addition to the driver, there were two passengers in the vehicle, both in the backside seats. The first run was made at the advisory speed through the length of curve. After driving through the curve at a particular speed, the same curve was also driven at the same speed but in the opposite direction. In each run, the speed was kept constant through the entire length of each curve. The

frequency of recording was four readings per second and ten readings per second in the ball-bank indicator and accelerometer, respectively.

3.4 Data Downloading

This section explains the way the raw data were collected simultaneously using both types of equipment. Furthermore, it provides an introduction to the software used in initial downloading and the computer settings.

3.4.1 Ball-bank indicator

Once the ball-bank indicator was set to collect the data, Microsoft Hyper Terminal program was started to download and save data in appropriate files. The Hyper Terminal popped up windows shown in Figures 3.12a and 3.12b were used for download setting. The first window displays the file name at the top left corner and the required laptop communication port number. If some extra device such as RS-232 adapter is being used, a number has to be assigned to that serial port. In this study, as the laptop had only two ports, one extra adapter was added, which provided extra connections. One of the adapter's ports was used to transfer data from ball-bank indicator to laptop. As soon as this setting was completed, another window appeared as shown in Figure 3.13.

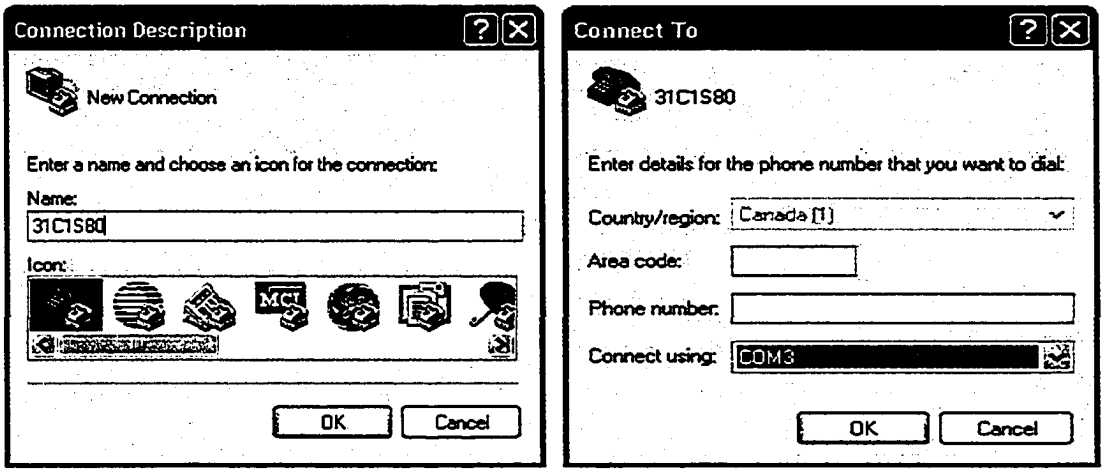

(a) First Connection Window **(b) Second Connection Window**

Figure 3.12: Hyper Terminal Setting Windows

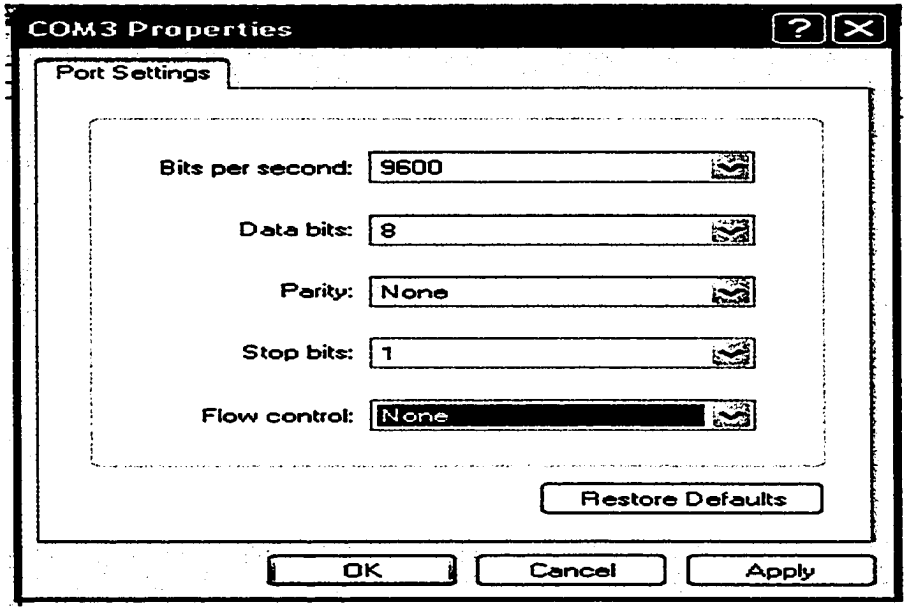

Figure 3.13: Port Setting Window

Figure 3.13 shows the popped up window used to change some default setting of Hyper Terminal to make it compatible for this study such as bit /sec and flow control etc. Finally, the ball-bank indicator was set to send data to the laptop

screen. This file was saved as a Hyper Terminal file on the hard drive of laptop. These saved files were moved to an Excel sheet for processing.

3.4.2 Corsa Accelerometer

Data collected through the Corsa accelerometer were first stored in the memory of the Corsa acquisition box. As soon as the data collection work of a segment was completed from one direction, the data were retrieved and sent to the laptop hard-drive. Through this procedure file saved in hard-drive could be opened in Corsa software. Moreover, opening a file in the Corsa software processed the data to be displayed in a graphical form like one shown below in Figure 3.14.

The data values can be seen by selecting "view" and then "data values" in the main menu while keeping the graphical presentation of data open on the laptop screen. This time, data values will appear in "dat" file format as shown in Figure 3.15. The same "dat" file can be exported to a "comma separated value" (CSV) file through "file" and "save" in the main menu. In this way, data are saved at assigned location as a "CSV" file. The CSV file can then be processed in Microsoft environment.

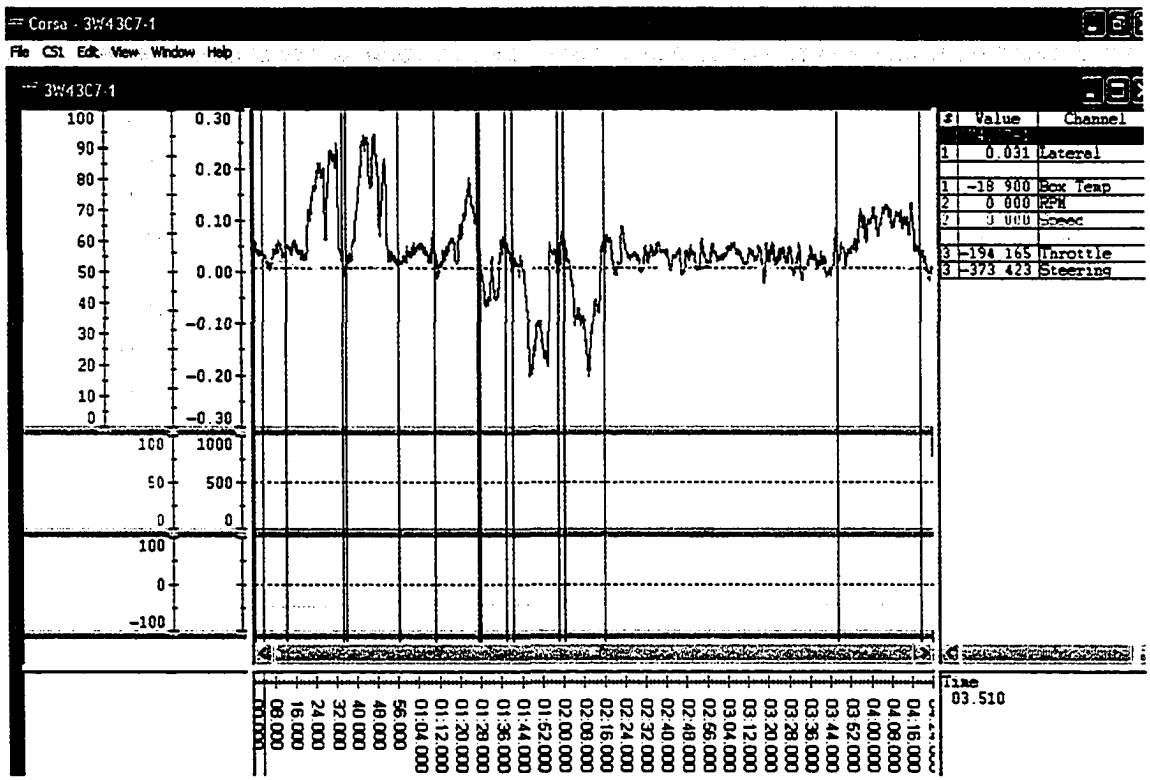

Figure 3.14: Data Acquisition Box's Output Data in Graphical Form

Data Values (3W43C7-1.dat)

Scaled Data Values

Time	Lateral	LonG	Box Temp	RPM	Speed	Brake	Throttle	Steering
00.000	0.022	0.096	-18.900	0.000	0.000	26.314	-194.165	-373.273
00.100	0.048	0.096						
00.200	0.048	0.096						
00.300	0.048	0.096						
00.400	0.046	0.096						
00.500	0.053	0.096						
00.600	0.046	0.094						
00.700	0.048	0.094						
00.800	0.048	0.101						
00.900	0.041	0.094						
01.000	0.050	0.092	-18.900			26.286	-194.064	-373.273
01.100	0.041	0.096						
01.200	0.036	0.094						
01.300	0.031	0.098						
01.400	0.029	0.092						
01.500	0.027	0.094						
01.600	0.034	0.089						
01.700	0.031	0.098						
01.800	0.036	0.094						
01.900	0.022	0.094						
02.000	0.034	0.092	-18.900			26.286	-194.165	-373.273
02.100	0.022	0.092						
02.200	0.034	0.094						
02.300	0.024	0.089						
02.400	0.031	0.089						
02.500	0.031	0.096						
02.600	0.024	0.096						
02.700	0.027	0.098						
02.800	0.031	0.101						
02.900	0.031	0.098						
03.000	0.027	0.098	-18.900			26.314	-194.064	-373.273
03.100	0.027	0.110						

Figure 3.15: Corsa Data file in .dat format

The number of values collected is possible to view by going to the "view" option in main menu and then choosing either "events" or "sets". In the same way the details of events that took place in each run while data were collected can also be seen. The required information can also be seen in tabular form as one shown below in Figure 3.16a and Figure 3.16b.

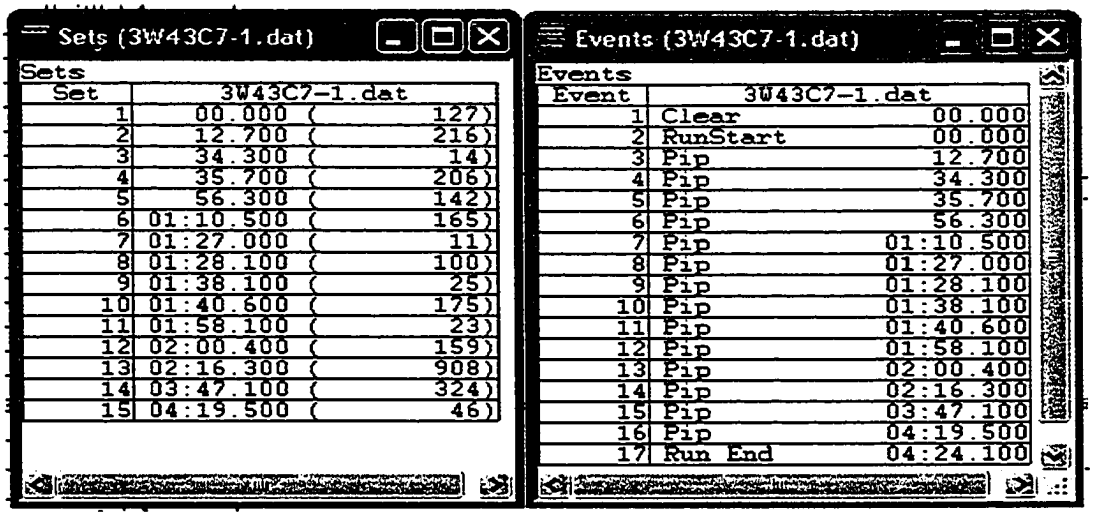

Sets (3W43C7-1.dat)

Sets

Set	3W43C7-1.dat	
1	00.000 (	127)
2	12.700 (	216)
3	34.300 (	14)
4	35.700 (	206)
5	56.300 (	142)
6	01:10.500 (	165)
7	01:27.000 (	11)
8	01:28.100 (	100)
9	01:38.100 (	25)
10	01:40.600 (	175)
11	01:58.100 (	23)
12	02:00.400 (	159)
13	02:16.300 (	908)
14	03:47.100 (	324)
15	04:19.500 (	46)

Events (3W43C7-1.dat)

Events

Event	3W43C7-1.dat	
1	Clear	00.000
2	RunStart	00.000
3	Pip	12.700
4	Pip	34.300
5	Pip	35.700
6	Pip	56.300
7	Pip	01:10.500
8	Pip	01:27.000
9	Pip	01:28.100
10	Pip	01:38.100
11	Pip	01:40.600
12	Pip	01:58.100
13	Pip	02:00.400
14	Pip	02:16.300
15	Pip	03:47.100
16	Pip	04:19.500
17	Run End	04:24.100

(a) Number of Values Collected **(b) Details of Events**

Figure 3.16: Corsa Sets and Events files in dat format

3.5 Field Notes

Field notes were compiled for each segment. These notes contained the geometric information of that segment. Information including the start point of the each run of each segment and its relative distance from start and end points of each curve were also recorded. These notes also contained date and time of data collection, weather of the day; and some geometric details of curves, which are not related to this study but are part of this segment. Furthermore, the notes contained details of all events such as interruption in data collection due to a

slow moving vehicle, traffic jam or equipment malfunction and part of the segment affected due to that factor.

Chapter 4
Data Processing

This chapter covers the details on the distribution of raw data into different files and its further processing for final analysis. Section 4.1 deals with the process of placing the data into different files, screening and correcting any disorder present. Section 4.2 presents the process of formatting of data for analysis.

4.1 Data Screening

After saving the data in Excel format the files were separated into two groups that corresponded to the ball-bank indicator data files and accelerometer data files. These files were screened carefully for any discrepancies as explained in the following sections.

4.1.1 Ball-Bank Indicator

The majority of the data were clearly understandable, and it was relatively easy to decipher the locations of curves with start and stop points. However in some files or sections of files, it was hard to locate the points joining tangent or spiral to curves or curves to a spiral or tangent. This was especially true when curves were in close proximity to one another. At the same time, some locations of curve data displayed highly variable values with negative and positive signs. In the below given Figure 4.1, the first column presents the correct form of data while the rest of four columns are show disordered data.

Column 1	Column 2	Column 3	Column 4	Column 5	Column 6
RESET -2.39 -2.14 -1.81 -1.96 -1.64 -1.55 -1.54 -1.80 -1.98 -1.35 -1.10 -1.04 -1.25 -2.00 -3.28 -3.50 -2.97 -2.18 -2.71 -3.07 -2.39 -2.15 -2.36 -2.68 -1.69 -1.61 -1.98 -1.72 -1.91 -1.37 -0.80 -0.77 -0.71 -0.69 -0.40 -0.34 LEFT -3.50 RIGHT +1.02	F 2.162.72 -1.363.25 -0.694.26 -0.575.92 + -1.457.38 R -2.608.06 0 -2.848.19 0 -2.657.48 0 -2.447.11 0 -1.987.02 0 -2.408.00 0 -1.838.99 0 -0.488.88 1 -0.057.18 1 +0.875.80 1 +0.896.83 1 -0.388.53 1 +0.139.37 0 +0.117.68 0 -0.965.65 0 -2.414.57 1 -1.734.92 1 -0.785.44 1 -0.396.22 1 -1.426.56 1	-3.23 +3 -2.51 +2 -2.14 +1 -1.98 +2 -1.92 +3 -1.59 +3 -1.12 +3 -0.91 +3 +0.04 +4 -0.42 +6 -1.28 +5 -1.69 +4 -0.92 +3 -1.29	+ 0. - 2.92 + 1. - 3.29 + 1. - 3.53 + 2. - 3.56 + 3. - 2.48 + 4. - 1.55 + 4. - 1.07 + 4. - 0.59 + 4. - 0.33 + 4. + 0.47 + 3. - 0.11 + 3. - 0.46 + 2. - 1.13 + 0. - 2.35 - 0	RESET +0.89 +0.64 +0.45 +0.47 +0.04 -0.84 -1.76 -2.43 -2.76 -2.89 -3.46 -4.14 -4.21 -4.02	+ -1.902.89 R -1.633. -1 -1.232. -1 -1.022. -1 -1.001. -1 -1.84FT -1 -1.19 -1 -0.71 -1 -0.88 -1 -0.88 -1 -0.37 -1 -0.00 -1 -0.30 -0

Figure 4.1: Correct and Disordered Data Values

In case of disordered data files, correct values were often hard to extract, and as such opinion of the manufacturer was sought. It was also important to understand the reasons for this disorder and determine a technique to get the right results. Regarding this disorder, there were four different types of values as follows:

1. Two decimal points instead of one (column 2).
2. Two different series of values in each alternate line (column 3 and 4).
3. Values were skipping in every alternate line (column 5).
4. In between the values there were letters or words (column 6 letter R or FT).

A detailed e-mail for technical help was sent to the head office of Rieker Electronics Inc. (the manufacturer of the ball-bank indicator). The e-mail contained the above given sample of data for explanation. The head office of Rieker Electronics Inc., replied that the "reason for this disorder is a timing issue and miscommunication in recording which causes leading start pulses and sign bit missing". This problem with the instrument caused other problems in data such as an extra letter between values, extra values, or wrong signs or missing data. However, these data can still be useable if screened carefully and extra letters, numbers or dots can be removed by following the actual pattern of values of each part of recording. According to the given directions, all the disordered values were screened and placed in relevant files.

4.1.2 Adding the Offset Value

The option of relative 0 (REL ON) was available in the ball-bank indicator but it needed to be activated each time the indicator is powered off/on and the car needed to be parked on level surface, which was not workable in this study. Specifically, while collecting the data on busy roads, it was hard to find a levelled surface each time. Ball-bank indicator is small equipment with all control and memory at same place. Touching it frequently creates slight differences in readings. The best way was to adjust and fix the instrument carefully on its final place and continue to collect data without touching it. Therefore, it was decided not to use this option, but to record the offset value of each day and add it into recorded values of that segment. Each day, prior to start of data collection, the vehicle would park on some level surface and the ball-bank indicator was set to get the value of ball-bank indicator in degrees when it is fitted in the car. As the offset values were the same each day (around -1.4 degrees), it was decided to consider 1.4 degrees (which comes to 0.024 in radian) as a common offset value, which was added to all values recorded using the ball-bank indicator.

4.1.3 Discarded Data

Disorders in the data of the ball-bank indicator mainly occurred in cases of data collection on Highways 43, 12, and 41. On Highway 41, the curves were too far from each other with construction activities just before and after some curves. Some portions of Highway 41 and 12 were located in built-up areas. Highway 12 also had problems of slow-moving vehicles and school activities. All these reasons were hindering the ball-bank indicator, which has limited memory, and

continued operation over a long period of time was difficult. The only option was frequent stops and starts, which would have produced also disturbance in data collection. Despite screening the data of these three highways, most of the curves ended up with missing values. In this situation, it was not possible to compare the ball-bank indicator data collected on these highways, to the accelerometer data. Therefore, the only option was to use the data collected from four Highways i.e. 31, 7, 15 and 17 for comparison to accelerometer data.

Highways 41 and 17 had construction activities at the time of data collection. Furthermore, there were busy intersections and newly installed traffic lights. All these factors made it difficult to record the data on five curves on Highway 41 and three curves on Highway 17.

As mentioned earlier the first driving speed was the posted speed of the highway, while the second and third speeds were 10 km/h more than the previous one. In the case of Highway 17, the posted speed was 90 km/h. Therefore, the selected driving speeds for this highway were 90, 100 and 110 km/h. Because the 110 km/h driving speed was unique for Highway 17 and data for comparison were not available from any other highway therefore, data recorded at speed of 110 km/h from Highway 17 were not included in analysis. The first driving speed for Highway 17 was 90 km/h therefore this Highway does not have any data of speed of 80 km/h.

4.1.4 Corsa Accelerometer

There were no significant problems with recorded values. Memory of DAB was enough to keep the accelerometer running for a longer period of time than

the ball-bank indicator. The lateral acceleration values recorded in this way were mixed with spiral and alignment data. It was hard to determine the values of the actual curve area among these several thousand values of each segment. The entire data were screened carefully to locate the position of the curves. The positions of each curve were marked and separated in different Excel sheets and graphs of these values were plotted beside them. Lateral acceleration values of the same curves recorded through the ball-bank indicator were also plotted for each curve in the same Excel sheets. Finally, graphs using the values of the ball-bank indicator and the accelerometer of same curve were compared to each other and if the patterns were similar, it was considered to be lateral acceleration values of that curve.

4.2 Data Formatting

Once the locations of different curves were identified in the recorded data using both types of equipment, it was possible to separate these values from spiral and alignment data.

4.2.1 Working with Ball-bank Indicator Data

Data collected through the ball-bank indicator were in degrees, while accelerometer data values of lateral acceleration were in g's. Therefore, the ball-bank data were converted from degrees to radians to bring them to the same unit.

Curve data recorded from both sources were kept separated using two sets of seven excel workbooks - one workbook for each highway from both

equipment. In these worksheets, length of each curve was also recorded besides lateral acceleration values. The start of a curve was marked as 0 meters while end of curve, as total length of that curve. In between, values of each row were calculated using Equation 4.1. This equation is based on the fact that in case of the ball-bank indicator, frequency of recordings was four values per second. Therefore, the increment in length in each row comes to:

$$\delta_{Lb} = v/4 \qquad (4.1)$$

δ_{Lb} = increment in length in each row of values in case of ball-bank indicator (m)

v = speed (m/sec) (22.22, 25.00 and 27.77 m/sec for speed 80, 90, 100 km/h respectively)

4.2.2 Working with Accelerometer Data

In the case of the accelerometer, data recording frequency was ten values per second. Therefore, the equation developed for increment of distance in each row of values comes to:

$$\delta_{La} = v/10 \qquad (4.2)$$

Here

δ_{La} = increment in length in each row of values in case of accelerometer (m)

v = speed (m/sec) (22.22, 25.00 and 27.77 m/sec for speed 80, 90, 100 km/h respectively)

Data collected through both the types of equipment consistently showed a difference in the values of lateral acceleration on right-turn and left-turn curves. It

was important to confirm that malfunction of devices is not the reason for this difference. The manufacturer i.e. Corsa Instruments Inc. was contacted and informed about the problem. The manufacturer suggested some measures. The most important one was to put this instrument on a table in laboratory and collect data from different directions by moving the table up and down and check if it is showing the same pattern. The final conclusion was that equipment is working well and recorded values are representing the actual lateral acceleration of that time.

4.2.3 Combining Accelerometer and Ball-bank Indicator Data

Data from both types of equipment for each highway were then combined in one Excel workbook. In this way, seven workbooks were prepared – one for each highway. Sheet 1 of each workbook was used to record the data collected north or east bound while sheet 2 contained the data for south or west bound. After combining the data, graphs of values of each curve and equipment were prepared and compared to each other. Finally, both graphs of each curve but from different equipment were combined in one graph for each curve to confirm that data collected through both types of equipment is showing the same pattern. This exercise was done to double check and make sure that all curves data were processed correctly so far, and there are no discrepancies. In the next stage, all data collected from each equipment were combined in a different workbook in a way that sheet 1 was showing data of all curves of each equipment in the north or east direction, while similar data from the same equipment but in the south or

west direction in other sheet. The same practice was repeated for the accelerometer data on two other sheets.

4.2.4 Calculating Mode, Median, Average Theoretical Lateral Acceleration

The data of all the curves were combined in seven workbooks, one for each highway. In each workbook, the first sheet was used to record data for all curves, all speeds and both equipment in long lines but in the north or east directions. The second sheet was used for same information, but in the south or west direction. At the bottom of each line of data: maximum, minimum, mode, median and average of each curve were calculated by using the Excel files tools. Finally, these values were moved to the main workbook. In that workbook, the first sheet was used for recording the data of all curves of all the highways but only one type of equipment in a continuous line. The second sheet was used for the same information but with other equipment. In this way, the entire data were recorded in six sheets of the same workbook. Beside these calculated values, geometric information of same curves was also recorded in the corresponding rows of the same sheet.

For the purpose of comparing the observed lateral acceleration to the theoretical lateral acceleration, theoretical lateral acceleration was calculated using the point mass equation (refer to Equation 3.2) as follows:

$$a_{th} = (V^2)/(127R) - e/100$$

where:

a_{th} = theoretical lateral acceleration (g)

V = speed (km/h)

R = radius of curve (m)

e = superelevation rate (percent)

4.2.5 Separating Data According to the Curve Directions

An obvious pattern observed during formatting of the data was that values of lateral acceleration are higher when the test vehicle turning right than driving on same curve and same speed but turning left. For the purpose of working more closely to this pattern, it was necessary to separate each curve data according to the driving directions. Therefore, average values of left-turn curves and right-turn curves were calculated and recorded in the separate columns for each driving speed and each type of equipment used.

4.2.6 Data Selection for Analysis

Data collected through the Corsa accelerometer having following advantages as compare to the ball-bank indicator:

1. Data of all highways and all curves selected for study were available for analysis.
2. Frequency of data collection was 10 readings per second as compared to 4 readings per second in case of the ball-bank indicator. Hence accelerometer's recorded data were having more values increasing the possibilities of accuracy.
3. Memory of data acquisition box of Corsa accelerometer was much greater than the ball-bank indicator. Therefore, data collected were not only of

curves but of the entire segment, which includes a spiral and tangent. These extra values of data helped identifying the exact locations of curves and spirals because of different types of pattern of lateral acceleration for spirals and curves.

4. It was easy to stop or start accelerometer whenever needed because the equipment control system was separate from rest of equipment. In case of the ball-bank indicator there were two basic problems: one was less memory and another one was the difficulty in stopping and starting again.

The above given advantages were not available in the case of ball-bank indicator which resulted in discarding data from Highways 41, 12, and 43. Therefore, it was decided that data collected through Corsa accelerometer would be used for analysis in this study.

Chapter 5
Data Analysis

This chapter describes the data analysis conducted in this study and is divided into three parts. Section 5.1 consists of the analysis of different patterns observed in lateral acceleration values from both directions and their relationship with theoretical lateral acceleration (point mass equation). Section 5.2 explains the reasons for different values of both directions, and methodology developed for analysis. Section 5.3 deals with development of statistical models for the prediction of lateral acceleration with uneven weight distribution.

5.1 Lateral Acceleration Results

In situations where the radius of a curve, driving speed and superelevation rate are the same, the lateral acceleration of a vehicle turning left or right should logically be equal in magnitude and opposite in direction. However, lateral acceleration data collected in this study clearly displayed a trend of higher values in the case of right-turn curves compared to left-turn curves. Although all data presented in this chapter correspond to the Corsa accelerometer, these patterns were eminent in both the ball-bank indicator and the Corsa accelerometer values. Furthermore, while comparing these values with theoretical lateral acceleration values (calculated using the point mass equation), neither direction produces results that are equal to the theoretical lateral acceleration (refer to Figure 5.1). The data presented in Table 5.1 reveal that trend of values of observed lateral acceleration in both directions.

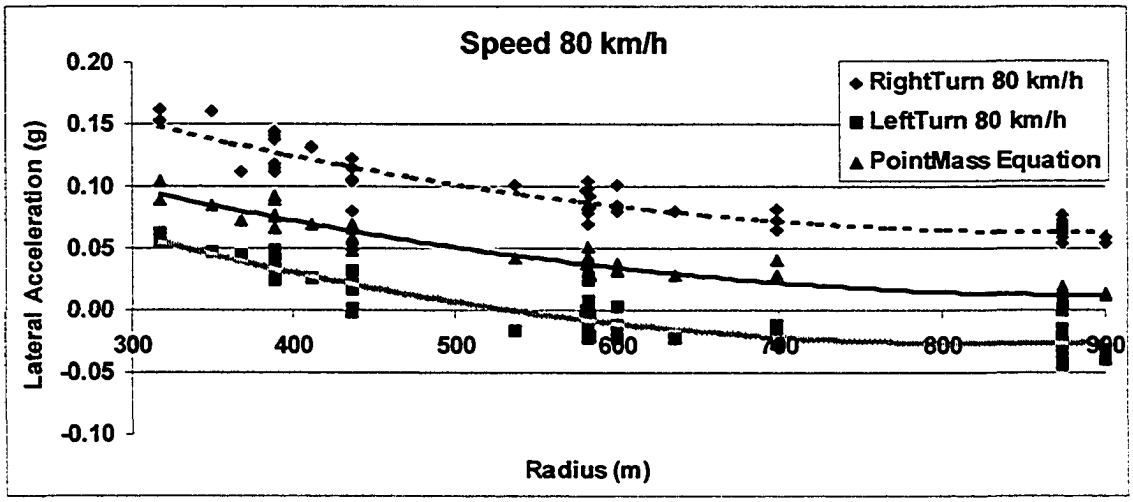

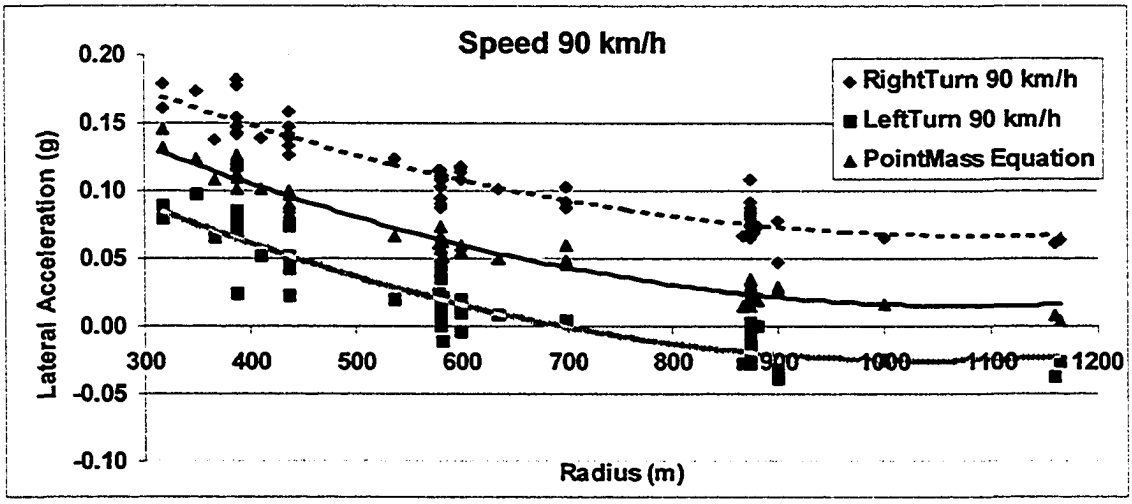

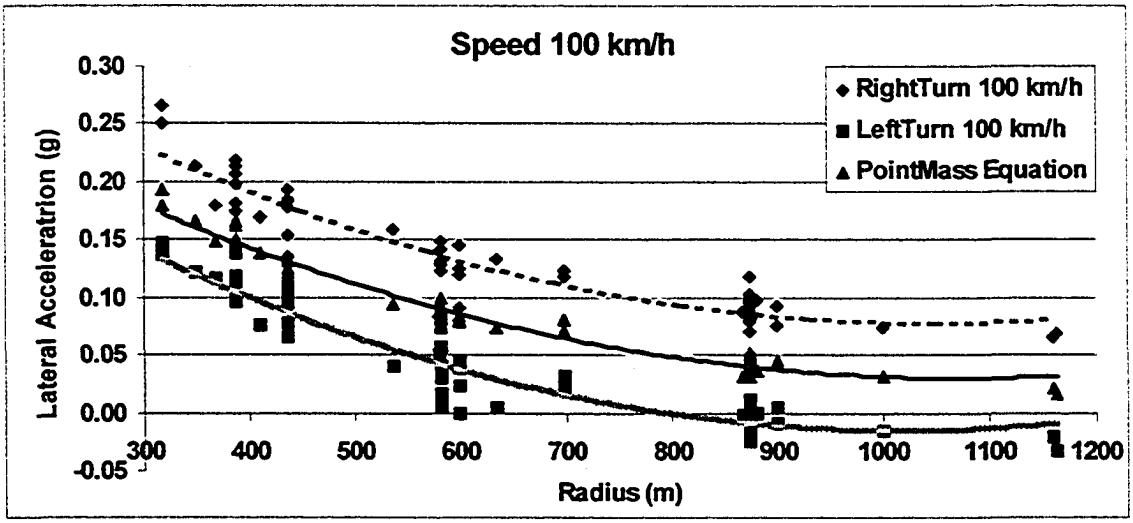

Figure 5.1 Observed v/s Theoretical Lateral Acceleration

Table 5.1: Observed Lateral Acceleration v/s Point Mass Equation

Geometric Features			Lateral Acceleration (80 km/h)				Lateral Acceleration (90 km/h)				Lateral Acceleration (100 km/h)			
High-way #	Radius (m)	Superele-vation (e)	Right Turn	Left Turn	Average (R+L)/2	Theore-Tical	Right Turn	Left Turn	Average (R+L)/2	Theore-tical	Right Turn	Left Turn	Average (R+L)/2	Theore-tical
12	317.510	0.055	0.163	-0.055	0.109	0.104	0.179	-0.089	0.134	0.146	0.265	-0.147	0.206	0.193
12	317.510	0.069	0.153	-0.062	0.108	0.090	0.161	-0.080	0.120	0.132	0.250	-0.137	0.194	0.179
31	349.000	0.060	0.160	-0.046	0.103	0.085	0.174	-0.098	0.136	0.123	0.213	-0.122	0.168	0.166
12	367.640	0.065	0.113	-0.044	0.078	0.072	0.137	-0.065	0.101	0.109	0.179	-0.117	0.148	0.150
31	388.000	0.064	0.138	-0.025	0.081	0.066	0.147	-0.023	0.085	0.101	0.207	-0.099	0.153	0.139
43	388.000	0.041	0.116	-0.038	0.077	0.089	0.155	-0.074	0.114	0.124	0.198	-0.117	0.157	0.162
43	388.000	0.055	0.118	-0.035	0.077	0.075	0.143	-0.085	0.114	0.110	0.181	-0.139	0.160	0.148
41	388.080	0.053	0.145	-0.038	0.091	0.077	0.182	-0.070	0.126	0.111	0.218	-0.096	0.157	0.150
41	388.080	0.052	0.141	-0.047	0.094	0.077	0.178	-0.082	0.130	0.112	0.214	-0.118	0.166	0.150
41	388.080	0.037	0.112	-0.048	0.080	0.093	0.142	-0.119	0.130	0.127	0.174	-0.113	0.144	0.166
7	410.913	0.054	0.131	-0.026	0.078	0.069	0.139	-0.052	0.096	0.102	0.169	-0.076	0.122	0.138
31	436.600	0.067	0.106	-0.019	0.063	0.048	0.133	-0.073	0.103	0.079	0.153	-0.095	0.124	0.113
7	436.592	0.049	0.080	-0.021	0.051	0.066	0.127	-0.023	0.075	0.097	0.135	-0.065	0.100	0.131
43	436.590	0.046	0.116	-0.031	0.074	0.069	0.139	-0.051	0.095	0.100	0.193	-0.107	0.150	0.134
43	436.590	0.063	0.105	-0.002	0.053	0.052	0.147	-0.048	0.098	0.083	0.178	-0.097	0.138	0.117
41	436.570	0.056	0.123	0.001	0.061	0.060	0.158	-0.041	0.100	0.090	0.184	-0.077	0.131	0.125
41	436.570	0.058	0.106	-0.017	0.062	0.057	0.141	-0.044	0.093	0.088	0.183	-0.102	0.143	0.122
41	537.340	0.052	0.101	0.016	0.042	0.042	0.124	-0.020	0.072	0.067	0.159	-0.040	0.100	0.094
31	580.000	0.049	0.097	0.000	0.049	0.038	0.116	-0.023	0.069	0.061	0.140	-0.049	0.095	0.087
15	582.125	0.060	0.098	0.013	0.042	0.026	0.088	-0.007	0.048	0.049	0.149	-0.030	0.090	0.075
7	582.125	0.042	0.104	-0.007	0.056	0.044	0.095	-0.018	0.056	0.067	0.132	-0.016	0.074	0.093
7	582.125	0.052	0.078	0.000	0.039	0.035	0.108	0.000	0.054	0.058	0.131	-0.040	0.085	0.084
7	582.125	0.060	0.082	0.022	0.030	0.027	0.103	-0.013	0.058	0.050	0.131	-0.005	0.068	0.075
43	582.120	0.053	0.070	0.006	0.032	0.034	0.090	-0.010	0.050	0.057	0.124	-0.037	0.081	0.082

Table 5.1: Observed Lateral Acceleration v/s Point Mass Equation (Continued)

Geometric Features			Lateral Acceleration (80 km/h)				Lateral Acceleration (90 km/h)				Lateral Acceleration (100 km/h)			
High-way #	Radius (m)	Superele-vation (e)	Right Turn	Left Turn	Average (R+L)/2	Theore-Tical	Right Turn	Left Turn	Average (R+L)/2	Theore-tical	Right Turn	Left Turn	Average (R+L)/2	Theore-tical
43	582.120	0.036	0.099	-0.024	0.061	0.051	0.115	-0.044	0.080	0.074	0.128	-0.081	0.104	0.099
41	582.100	0.046	0.084	-0.004	0.044	0.040	0.111	-0.035	0.073	0.063	0.128	-0.041	0.084	0.089
31	583.000	0.057	0.092	0.022	0.035	0.029	0.108	0.011	0.049	0.052	0.132	-0.013	0.073	0.078
31	583.000	0.048	0.083	0.004	0.039	0.039	0.111	-0.021	0.066	0.062	0.141	-0.057	0.099	0.088
15	600.000	0.051	0.085	0.012	0.036	0.033	0.113	0.004	0.055	0.056	0.125	-0.038	0.082	0.081
15	600.000	0.047	0.102	0.013	0.045	0.037	0.117	-0.012	0.065	0.060	0.145	-0.023	0.084	0.085
15	600.000	0.051	0.081	0.023	0.029	0.033	0.118	-0.010	0.064	0.056	0.092	0.000	0.046	0.081
15	600.000	0.052	0.083	-0.003	0.043	0.032	0.109	-0.020	0.064	0.055	0.121	-0.045	0.083	0.080
41	635.040	0.051	0.080	0.023	0.028	0.029	0.102	-0.008	0.055	0.050	0.134	-0.004	0.069	0.073
7	698.550	0.045	0.082	0.020	0.031	0.027	0.103	-0.004	0.054	0.046	N/A	N/A	N/A	N/A
12	698.510	0.032	0.073	0.012	0.030	0.041	0.087	-0.003	0.045	0.060	0.124	-0.031	0.077	0.081
12	698.510	0.043	0.065	0.027	0.019	0.029	0.092	-0.003	0.048	0.048	0.119	-0.022	0.070	0.070
17	866.000	0.059	N/A	NA	N/A	N/A	0.066	0.028	0.019	0.015	0.087	0.002	0.042	0.032
31	873.200	0.044	0.065	0.017	0.024	0.013	0.092	0.012	0.040	0.029	0.079	-0.007	0.043	0.046
31	873.200	0.053	0.059	0.044	0.008	0.005	0.082	0.023	0.030	0.020	0.070	0.022	0.024	0.037
31	873.200	0.043	0.073	0.035	0.019	0.014	0.083	0.014	0.034	0.030	0.103	0.017	0.043	0.047
31	873.200	0.044	0.062	0.022	0.020	0.013	0.081	0.005	0.038	0.029	0.097	-0.010	0.054	0.046
15	873.188	0.038	0.066	0.030	0.018	0.020	0.108	0.026	0.041	0.035	0.119	0.025	0.047	0.052
15	873.188	0.042	0.068	0.015	0.026	0.015	0.068	-0.002	0.035	0.031	0.082	0.005	0.039	0.048
15	873.188	0.049	0.063	0.016	0.023	0.009	0.079	0.006	0.037	0.024	0.094	-0.009	0.051	0.041
7	873.188	0.040	0.070	0.023	0.023	0.018	0.079	0.021	0.029	0.033	0.087	0.004	0.042	0.050
7	873.188	0.049	0.054	0.036	0.009	0.008	0.085	0.025	0.030	0.024	0.097	-0.002	0.050	0.041
7	873.188	0.045	0.066	0.029	0.019	0.013	0.088	0.028	0.030	0.028	0.092	0.004	0.044	0.045
7	873.188	0.047	0.063	0.042	0.010	0.010	0.075	0.022	0.027	0.026	0.098	0.003	0.047	0.043

Table 5.1: Observed Lateral Acceleration v/s Point Mass Equation (Continued)

Geometric Features			Lateral Acceleration (80 km/h)				Lateral Acceleration (90 km/h)				Lateral Acceleration (100 km/h)			
High-way#	Radius (m)	Superele-vation (e)	Right Turn	Left Turn	Average (R+L)/2	Theore-Tical	Right Turn	Left Turn	Average (R+L)/2	Theore-tical	Right Turn	Left Turn	Average (R+L)/2	Theore-tical
43	873.190	0.049	0.059	0.022	0.018	0.008	0.079	0.013	0.033	0.024	0.092	-0.002	0.047	0.041
41	873.150	0.050	0.078	0.000	0.039	0.008	0.070	0.000	0.035	0.023	0.050	0.000	0.025	0.041
41	873.150	0.058	0.055	0.000	0.027	0.000	0.065	0.000	0.032	0.015	0.099	0.000	0.049	0.032
41	873.180	0.039	0.059	0.027	0.016	0.019	0.073	0.010	0.032	0.034	0.093	-0.001	0.047	0.052
17	876.000	0.049	N/A	N/A	N/A	N/A	0.069	0.000	0.034	0.024	0.082	0.000	0.041	0.041
17	880.000	0.052	N/A	N/A	N/A	N/A	0.073	0.000	0.036	0.020	0.099	0.000	0.049	0.037
15	900.000	0.042	0.054	0.032	0.011	0.014	0.077	0.032	0.023	0.029	0.092	-0.004	0.048	0.046
15	900.000	0.044	0.059	0.039	0.010	0.012	0.047	0.039	0.004	0.027	0.076	0.009	0.034	0.044
17	1000.000	0.047	N/A	N/A	N/A	N/A	0.065	0.025	0.020	0.016	0.074	0.016	0.029	0.031
17	1160.000	0.046	N/A	N/A	N/A	N/A	0.062	0.038	0.012	0.009	0.066	0.021	0.022	0.022
17	1164.000	0.051	N/A	N/A	N/A	N/A	0.064	0.027	0.019	0.004	0.070	0.034	0.018	0.017

As stated in the literature review, Felipe and Navin (1998) observed this pattern due to change in direction in a different context. They stated "It was found that the speeds selected by the drivers were higher when the small curves were driven counter-clockwise (i.e. left turn) rather than clockwise (i.e. right turn)". The study of Felipe and Navin focused on the relationship between speeds and curve radii and did not consider the lateral acceleration as a contributing factor in speeds selection. There is a possibility that drivers turning left would feel more comfortable due to lower lateral acceleration and would adopt higher speeds than drivers as opposed to ones turning right.

The AASHTO Green book recommends the point mass equation for calculating the theoretical values of lateral acceleration on highway curves (refer to Equation 3.2). This study also used the same equation to calculate the lateral acceleration at different speeds and curve radii. The relationship between theoretical values of lateral acceleration and observed lateral acceleration at the site from both directions was analyzed in the following section.

5.2 Effect of Turning Direction

This section explains the reason for different values of lateral acceleration recorded in right-turn curves compared to left-turn curves. In this section, methodology and new equations are developed for theoretical analysis of available data. At the end, collected data were used to prove if methodology being developed is correct.

5.2.1 Static Weight and Driving Direction

The preliminary investigation of collected data coupled with thorough study of literature led to the conclusion that the uneven weight due to seating arrangement of the occupants of the test vehicle is causing extra load on the driver side and ultimately reflecting as difference in values of lateral acceleration. During data collection, the test vehicle had just the driver in front portion and his weight was 105 kg (234 lbs). The passenger seat beside driver was kept empty because of the accelerometer, which was fitted on the backside of this seat. In the rear, there were two passengers. Again, the left side passenger was of 80 kg weight while weight of the passenger on the right side was 65 kg. Besides these weights, there was a 12 kg weight of instruments and luggage on each side of test vehicle (left and right). All these weights when added were making a difference of 120 kg access on the driver side as compared to the other side (refer to Figure 5.2).

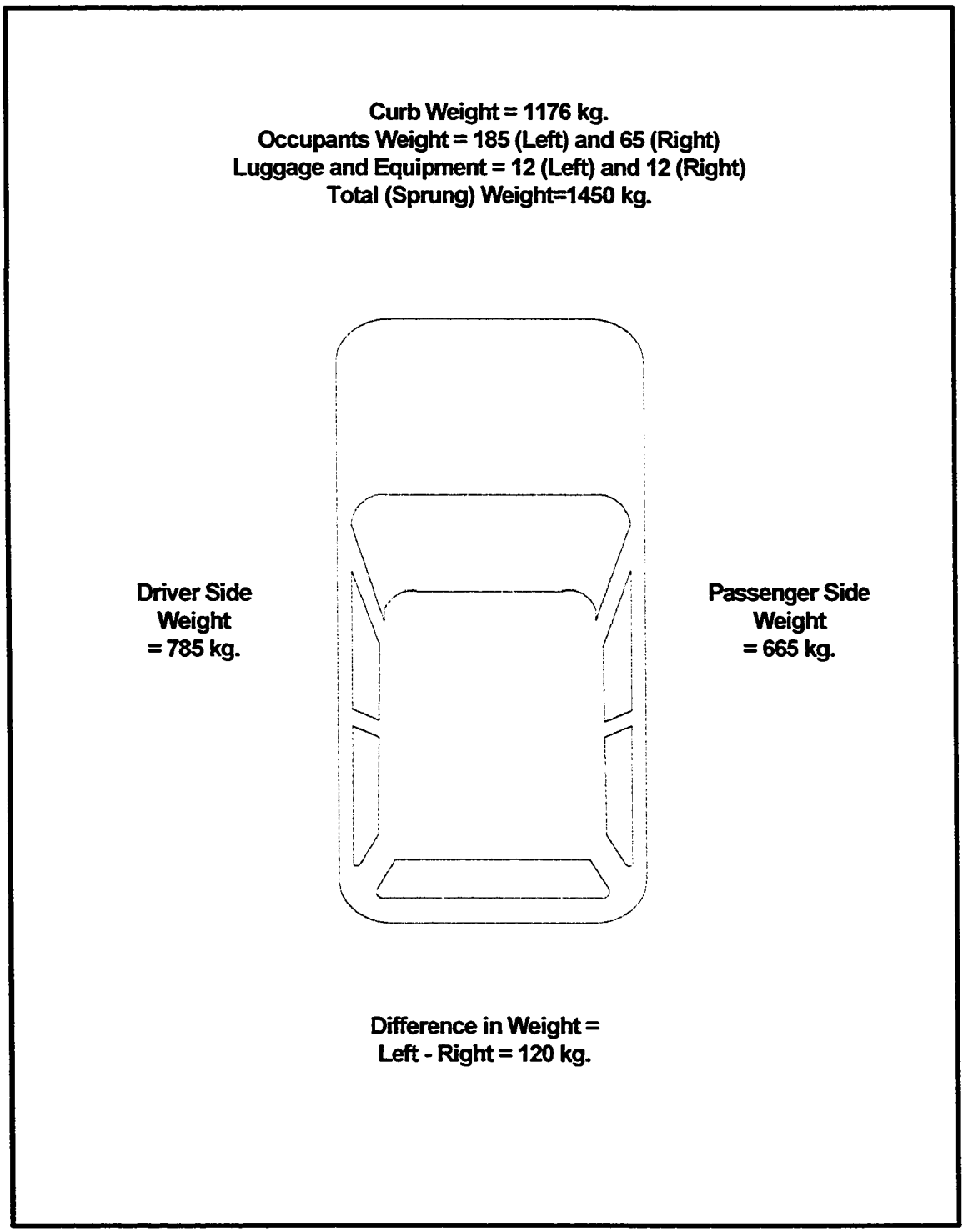

Figure 5.2: Distribution of Load on Different Wheels

The total weight including static weight on the outer wheels (W_{sw}) in the case of a right-turn curve is 785 kg. On the other side, the weight on the outer wheels (W_{sw}) is 685 kg in the case of left-turn curves. This difference in weight between left and right side curves causes a static roll angle (p_s), which ultimately affects the values of lateral acceleration collected from both directions.

5.2.2 Effect of Static Weight

If the vehicle is turning right and the road is superelevated, in this situation the driver side has more weight than the opposite side. The driver (or outer) side side will have three types of weights: the weight transfer from the inside wheels due to lateral acceleration, the weight transfer due to body roll, and the available static weight on this side. The excess static weight on this side will cause the lateral acceleration to be higher than in the case of left turn.

In contrary, when vehicle is turning left the driver side will be towards centre of the curve or opposite to the outer wheels and also this side will be down as compare to other side due to the superelevation. Hence, total weight on the outer side wheels will clearly be less than first case due to lack of static weight. Therefore, lateral acceleration generated in this side will clearly be less than opposite side. As such the static weight on driver side affected the lateral acceleration generated in left-side curve. This condition caused less amount of lateral acceleration at this side. Now if the static weight can be converted into lateral acceleration then by subtracting twice of it to the right turning values the net result should be similar to opposite side values of lateral acceleration (refer to Figure 5.3).

By further working with this static weight due to seating arrangement in side the vehicle, an equation can be developed as follows:

$$\theta_R = \alpha_R + e - \rho_S - \rho_D \quad (5.1)$$

$$\theta_L = \alpha_L + e + \rho_S - \rho_D \quad (5.2)$$

by subtracting (5.2) from (5.1)

$$\theta_R - \theta_L = \alpha_R - \alpha_L - 2\rho_S$$

$$\alpha_R - \alpha_L = 2\rho_S \quad (5.3)$$

where:

θ_R = total lateral acceleration angle at right-turn curves

θ_L = total lateral acceleration angle at left-turn curves

α_R = net lateral acceleration angle at right-turn curves

α_L = net lateral acceleration angle at left turn-curves

e = superelevation rate

ρ_S = static roll angle due to static weight

ρ_D = dynamic roll angle due to body roll

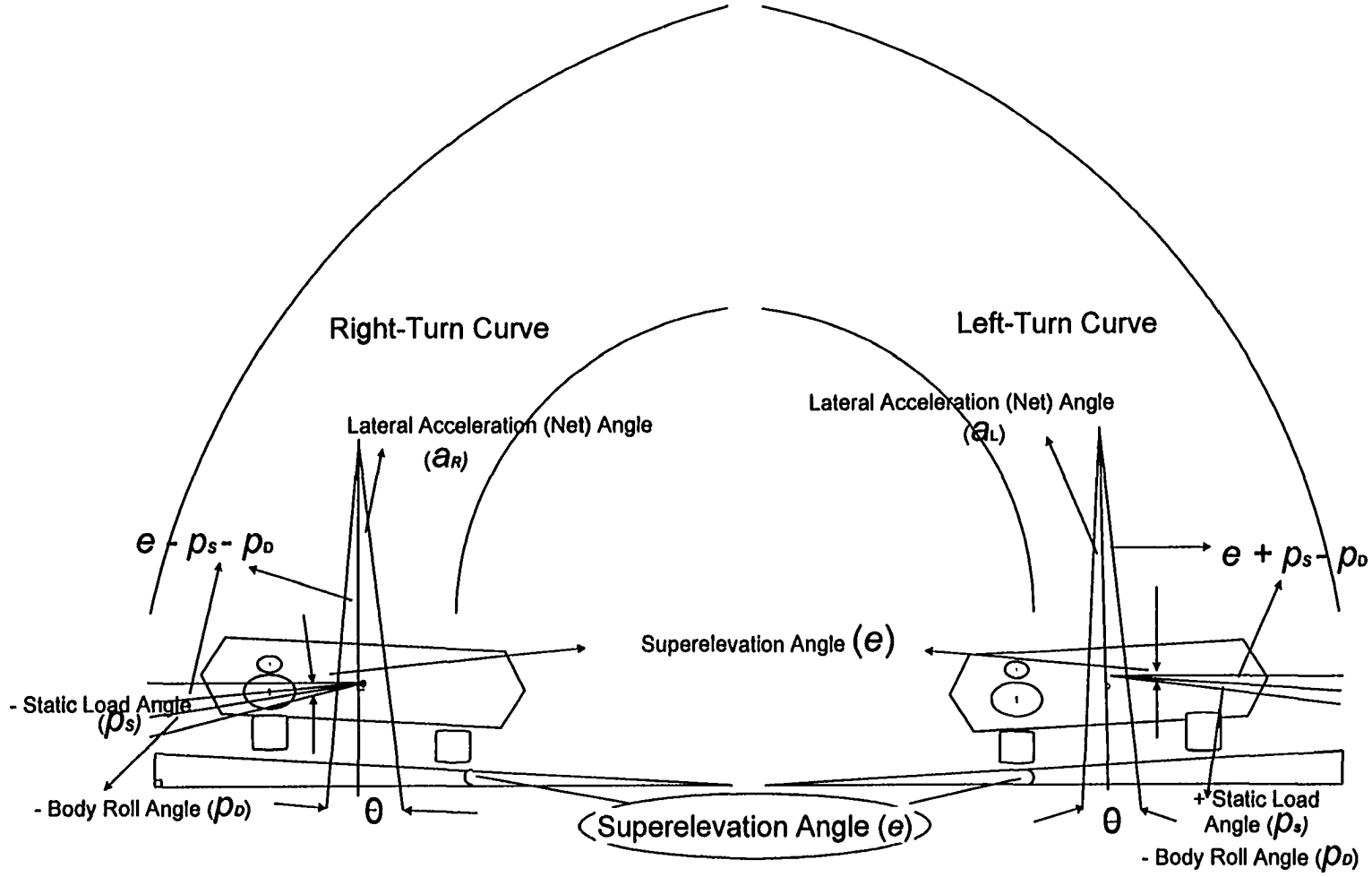

Figure 5.3: Curve Driving from Different Directions

5.2.3 Static Roll Angle

The value of static roll angle has been calculated using Equation 5.3. Table 5.2 is presenting the values of static roll angle used in this analysis. Figure 5.4 is presenting the effect of different speeds on static roll angle at different curve radii. It can be seen that neither there is any significant gap between static roll angles values at different speeds nor curve radii affect static roll angle. The descriptive statistics (refer to Table 5.3) present mean value of 0.046 and standard deviation value of 0.009, which are not close to each other thus a sign, that distribution of data is reasonably symmetrical about the mean. The ranges of ± one, ± two and ± three standard deviation are 0.037 to 0.055, 0.028 to 0.064 and 0.019 to 0.073 respectively. The percentages of calculated values of static roll angle falling in these ranges are 63%, 96% and 99%, which are very similar to the percentages specified for normal distribution values (68%, 95% and 99%). This is another sign that distribution of data is reasonably symmetrical about the mean. In Table 5.3 skewness value is -0.312 and its corresponding standard error is 0.186. The range of ± twice of standard error comes to -0.372 to +0.372. The value of skewness falls within this range, which shows that skewness is within the expected range of chance fluctuation, and indicates a distribution with no significant skewness problem. The Kurtosis value is 1.079 and its corresponding standard error is 0.37. The twice of standard error i.e. 0.74 is less than kurtosis value which is positive in this case. This positive value indicates a relatively peaked distribution (that is, too tall) as compared to the normal distribution.

Table 5.2: Effect of Speeds on Static Roll Angle

Lateral Acceleration Observed (g)							Static Roll Angle		
Radius	80 km/h		90 km/h		100 km/h		(Right+Left)/2		
(m)	Right Turn	Left Turn	Right Turn	Left Turn	Right Turn	Left Turn	80 km/h	90 km/h	100 km/h
317.5	0.163	-0.055	0.179	-0.089	0.265	-0.147	0.054	0.045	0.059
317.5	0.153	-0.062	0.161	-0.080	0.250	-0.137	0.046	0.041	0.056
349.0	0.160	-0.046	0.174	-0.098	0.213	-0.122	0.057	0.038	0.046
367.6	0.113	-0.044	0.137	-0.065	0.179	-0.117	0.035	0.036	0.031
388.0	0.138	-0.025	0.147	-0.023	0.207	-0.099	0.057	0.062	0.054
388.0	0.116	-0.038	0.155	-0.074	0.198	-0.117	0.039	0.040	0.041
388.0	0.118	-0.035	0.143	-0.085	0.181	-0.139	0.042	0.029	0.021
388.1	0.145	-0.038	0.182	-0.070	0.218	-0.096	0.053	0.056	0.061
388.1	0.141	-0.047	0.178	-0.082	0.214	-0.118	0.047	0.048	0.048
388.1	0.112	-0.048	0.142	-0.119	0.174	-0.113	0.032	0.011	0.031
410.9	0.131	-0.026	0.139	-0.052	0.169	-0.076	0.053	0.043	0.046
436.6	0.106	-0.019	0.133	-0.073	0.153	-0.095	0.044	0.030	0.029
436.6	0.080	-0.021	0.127	-0.023	0.135	-0.065	0.030	0.052	0.035
436.6	0.116	-0.031	0.139	-0.051	0.193	-0.107	0.042	0.044	0.043
436.6	0.105	-0.002	0.147	-0.048	0.178	-0.097	0.051	0.049	0.040
436.6	0.123	0.001	0.158	-0.041	0.184	-0.077	0.062	0.058	0.053
436.6	0.106	-0.017	0.141	-0.044	0.183	-0.102	0.045	0.049	0.041
537.3	0.101	0.016	0.124	-0.020	0.159	-0.040	0.058	0.052	0.060
580.0	0.097	0.000	0.116	-0.023	0.140	-0.049	0.048	0.046	0.045
582.1	0.098	0.013	0.088	-0.007	0.149	-0.030	0.056	0.040	0.060
582.1	0.104	-0.007	0.095	-0.018	0.132	-0.016	0.048	0.039	0.058
582.1	0.078	0.000	0.108	0.000	0.131	-0.040	0.039	0.054	0.046
582.1	0.082	0.022	0.103	-0.013	0.131	-0.005	0.052	0.045	0.063
582.1	0.070	0.006	0.090	-0.010	0.124	-0.037	0.038	0.040	0.043
582.1	0.099	-0.024	0.115	-0.044	0.128	-0.081	0.037	0.036	0.023
582.1	0.084	-0.004	0.111	-0.035	0.128	-0.041	0.040	0.038	0.044
583.0	0.092	0.022	0.108	0.011	0.132	-0.013	0.057	0.060	0.059
583.0	0.083	0.004	0.111	-0.021	0.141	-0.057	0.043	0.045	0.042
600.0	0.085	0.012	0.113	0.004	0.125	-0.038	0.048	0.059	0.043
600.0	0.102	0.013	0.117	-0.012	0.145	-0.023	0.057	0.052	0.061
600.0	0.081	0.023	0.118	-0.010	0.092	0.000	0.052	0.054	0.046
600.0	0.083	-0.003	0.109	-0.020	0.121	-0.045	0.040	0.044	0.038
635.0	0.080	0.023	0.102	-0.008	0.134	-0.004	0.054	0.045	0.059
698.6	0.082	0.020	0.103	-0.004	N/A	N/A	0.046	0.041	N/A
698.5	0.073	0.012	0.087	-0.003	0.124	-0.031	0.057	0.038	0.046
698.5	0.065	0.027	0.092	-0.003	0.119	-0.022	0.035	0.036	0.031

Table 5.2: Effect of Speeds on Static Roll Angle (Continued)

Lateral Acceleration Observed (g)							Static Roll Angle		
Radius	80 km/h		90 km/h		100 km/h		(Rigth+Left)/2		
(m)	Right Turn	Left Turn	Right Turn	Left Turn	Right Turn	Left Turn	80 km/h	90 km/h	100 km/h
866.0	N/A	N/A	0.066	0.028	0.087	0.002	N/A	0.062	0.054
873.2	0.065	0.017	0.092	0.012	0.079	-0.007	0.039	0.040	0.041
873.2	0.059	0.044	0.082	0.023	0.070	0.022	0.042	0.029	0.021
873.2	0.073	0.035	0.083	0.014	0.103	0.017	0.053	0.056	0.061
873.2	0.062	0.022	0.081	0.005	0.097	-0.010	0.047	0.048	0.048
873.2	0.066	0.030	0.108	0.026	0.119	0.025	0.032	0.011	0.031
873.2	0.068	0.015	0.068	-0.002	0.082	0.005	0.053	0.043	0.046
873.2	0.063	0.016	0.079	0.006	0.094	-0.009	0.044	0.030	0.029
873.2	0.070	0.023	0.079	0.021	0.087	0.004	0.030	0.052	0.035
873.2	0.054	0.036	0.085	0.025	0.097	-0.002	0.042	0.044	0.043
873.2	0.066	0.029	0.088	0.028	0.092	0.004	0.051	0.049	0.040
873.2	0.063	0.042	0.075	0.022	0.098	0.003	0.062	0.058	0.053
873.2	0.059	0.022	0.079	0.013	0.092	-0.002	0.045	0.049	0.041
873.2	0.078	0.000	0.070	0.000	0.050	0.000	0.058	0.052	0.060
873.2	0.055	0.000	0.065	0.000	0.099	0.000	0.048	0.046	0.045
873.2	0.059	0.027	0.073	0.010	0.093	-0.001	0.056	0.040	0.060
876.0	N/A	N/A	0.069	0.000	0.082	0.000	N/A	0.039	0.058
880.0	N/A	N/A	0.073	0.000	0.099	0.000	N/A	0.054	0.046
900.0	0.054	0.032	0.077	0.032	0.092	-0.004	0.052	0.045	0.063
900.0	0.059	0.039	0.047	0.039	0.076	0.009	0.038	0.040	0.043
1000.0	N/A	N/A	0.065	0.025	0.074	0.016	N/A	0.036	0.023
1160.0	N/A	N/A	0.062	0.038	0.066	0.021	N/A	0.038	0.044
1164.0	N/A	N/A	0.064	0.027	0.070	0.034	N/A	0.060	0.059

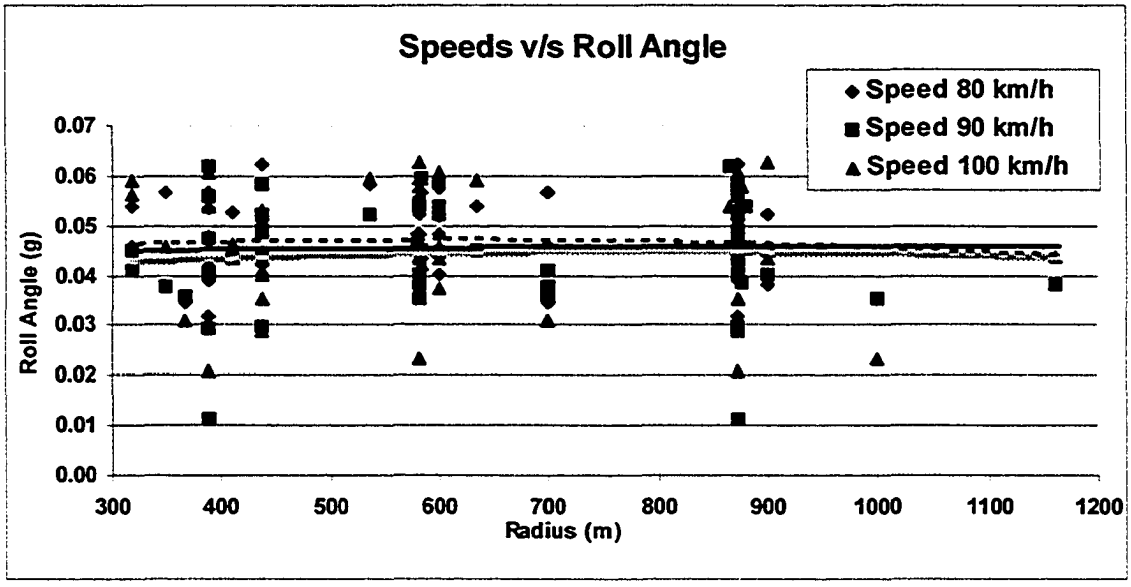

Figure 5.4: Effect of Speeds on Static Roll Angle for Different Radius

Table 5.3: Descriptive Statistics- Static Roll Angle

						Skewness		Kurtosis	
	N	Min	Max	Mean	Std. Deviation	Statistic	Std. Error	Statistic	Std. Error
Static Roll Angle	170	.012	.072	.0460	.0091	-.312	.186	1.079	.370

5.2.4 ANOVA Test of Static Roll Angle

One-way Analysis of Variance (ANOVA) was carried out to examine the effect of speed on static roll angle and to test the null hypothesis that the mean values of static roll angle corresponding to different driving speeds are equal. Observed *p*-value is 0.853, which is greater than critical value of 0.05. It shows that difference between means is not great enough and hence effect of speed on static roll angle is non-significant. Furthermore, the observed value of *F-ratio* (F_{obs}) is 0.159, which is less than the critical value of *F-ratio* (F_{crit}) i.e. 3.06 ($F_{(2,167,0.95)}$: degree of freedom for numerator is 2, degree of freedom for denominator is 167 and p_{crit} is 0.05). The F_{obs} shows that means are not significantly different which mean no effect of speed is discovered and null hypothesis is accepted. Therefore, ANOVA result confirmed that static roll angle is not affected by speed.

5.2.5 Average Observed versus Theoretical Lateral Acceleration

The values of lateral acceleration from opposite directions were added and average values were calculated for each corresponding radius of curve, speed and direction. All the average values of lateral acceleration were compared with theoretical lateral acceleration (refer to Table 5.1). The graphical presentation of these average values and theoretical lateral acceleration calculated using point mass equation could be seen in Figure 5.5.

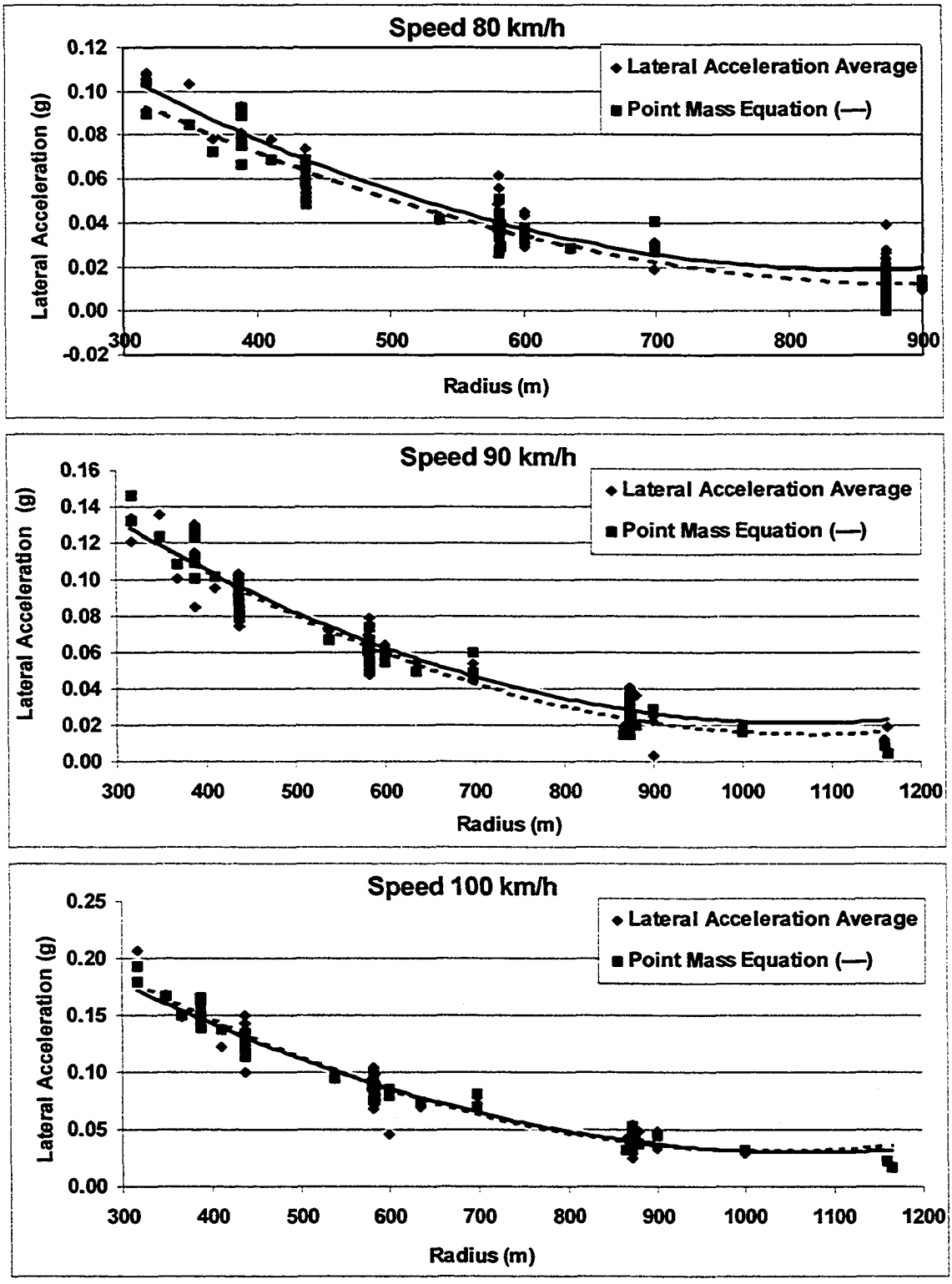

Figure 5.5 Average Observed v/s Theoretical Lateral Acceleration

Supplied data in Table 5.1 and its graphical presentation in Figure 5.5, for each driving speed separately depict the same trend in both types of lateral accelerations. This trend is clearly verifying the following points presented in the literature review (Lamm et al. 1991):

1. Lateral acceleration increases with increasing degree of curve.
2. Theoretical lateral acceleration is lower than observed lateral acceleration at the operating speeds of 80 km/h.
3. The gap between theoretical and observed lateral acceleration increase with decreasing operating speed.

The above-mentioned presentation illustrates that due to static roll angle, lateral acceleration in left-turn curves is less than right-turn curves. However, the average observed lateral acceleration for both direction comes close to the theoretical value. Thus, it can be seen that the excess value of observed lateral acceleration over the theoretical lateral acceleration in right-turn curves is close to the excess value of theoretical lateral acceleration over the observed lateral acceleration in left-turn curves. This similarity between the average observed lateral acceleration of both directions and theoretical lateral acceleration confirms the role of the static roll, which is not considered in highway design.

5.2.6 Effect of Dynamic Roll Angle

The difference between observed and theoretical lateral acceleration is due to dynamic roll angle (p_D). By referring back to Equations 5.1 and 5.2 and adding them:

$$\theta_R + \theta_L = \alpha_R + \alpha_L + 2e - 2\rho_D \qquad (5.4)$$

therefore

$$(\theta_R + \theta_L)/2 = (\alpha_R + \alpha_L)/2 + e - \rho_D$$

or

$$[(\theta_R + \theta_L)/2] - e = [(\alpha_R + \alpha_L)/2] - \rho_D$$

here

$[(\theta_R + \theta_L)/2] - e =$ theoretical net lateral acceleration (5.5)

and

$(\alpha_R + \alpha_L)/2 =$ observed average lateral acceleration (5.6)

Therefore equation 5.6 could be written as:

$$\alpha_{th} = \alpha_{av} - \rho_D$$

or

$$\alpha_{av} - \alpha_{th} = \rho_D \qquad (5.7)$$

The values of roll angle dynamic for different speeds of curves were calculated which could be seen in Table 5.4. The graphs showing the effect of speeds on absolute values of dynamic roll angle can also be seen in Figure 5.6.

Table 5.4: Dynamic Roll Angle at Different Speeds

	80 km/h			90 km/h			100 km/h		
Radius (m)	Average Observed	Theor-etical	Roll Angle Dynamic	Average Observed	Theor-etical	Roll Angle Dynamics	Average Observed	Theor-etical	Roll Angle Dynamics
317.5	0.109	0.104	0.005	0.134	0.146	-0.013	0.206	0.193	0.013
317.5	0.108	0.090	0.018	0.120	0.132	-0.012	0.194	0.179	0.014
349.0	0.103	0.085	0.018	0.136	0.123	0.013	0.168	0.166	0.002
367.6	0.078	0.072	0.006	0.101	0.109	-0.008	0.148	0.150	-0.002
388.0	0.081	0.066	0.015	0.085	0.101	-0.016	0.153	0.139	0.014
388.0	0.077	0.089	-0.012	0.114	0.124	-0.009	0.157	0.162	-0.005
388.0	0.077	0.075	0.002	0.114	0.110	0.004	0.160	0.148	0.012
388.1	0.091	0.077	0.014	0.126	0.111	0.015	0.157	0.150	0.007
388.1	0.094	0.077	0.016	0.130	0.112	0.018	0.166	0.150	0.015
388.1	0.080	0.093	-0.013	0.130	0.127	0.003	0.144	0.166	-0.022
410.9	0.078	0.069	0.009	0.096	0.102	-0.006	0.122	0.138	-0.016
436.6	0.063	0.048	0.014	0.103	0.079	0.024	0.124	0.113	0.011
436.6	0.051	0.066	-0.016	0.075	0.097	-0.022	0.100	0.131	-0.031
436.6	0.074	0.069	0.005	0.095	0.100	-0.005	0.150	0.134	0.016
436.6	0.053	0.052	0.001	0.098	0.083	0.015	0.138	0.117	0.020
436.6	0.061	0.060	0.001	0.100	0.090	0.009	0.131	0.125	0.006
436.6	0.062	0.057	0.004	0.093	0.088	0.005	0.143	0.122	0.020
537.3	0.042	0.042	0.001	0.072	0.067	0.005	0.100	0.094	0.005
580.0	0.049	0.038	0.011	0.069	0.061	0.008	0.095	0.087	0.008
582.1	0.042	0.026	0.016	0.048	0.049	-0.002	0.090	0.075	0.015
582.1	0.056	0.044	0.011	0.056	0.067	-0.011	0.074	0.093	-0.019
582.1	0.039	0.035	0.004	0.054	0.058	-0.004	0.085	0.084	0.002
582.1	0.030	0.027	0.003	0.058	0.050	0.009	0.068	0.075	-0.007
582.1	0.032	0.034	-0.002	0.050	0.057	-0.006	0.081	0.082	-0.002
582.1	0.061	0.051	0.011	0.080	0.074	0.006	0.104	0.099	0.005
582.1	0.044	0.040	0.003	0.073	0.063	0.010	0.084	0.089	-0.005
583.0	0.035	0.029	0.006	0.049	0.052	-0.003	0.073	0.078	-0.005
583.0	0.039	0.039	0.001	0.066	0.062	0.004	0.099	0.088	0.011
600.0	0.036	0.033	0.003	0.055	0.056	-0.001	0.082	0.081	0.001
600.0	0.045	0.037	0.007	0.065	0.060	0.005	0.084	0.085	-0.001
600.0	0.029	0.033	-0.004	0.064	0.056	0.008	0.046	0.081	-0.035
600.0	0.043	0.032	0.011	0.064	0.055	0.010	0.083	0.080	0.003
635.0	0.028	0.029	0.000	0.055	0.050	0.005	0.069	0.073	-0.004
698.6	0.031	0.027	0.004	0.054	0.046	0.008	N/A	N/A	N/A
698.5	0.030	0.041	-0.010	0.045	0.060	-0.015	0.077	0.081	-0.004
698.5	0.019	0.029	-0.011	0.048	0.048	-0.001	0.070	0.070	0.000
866.0	N/A	N/A	N/A	0.019	0.015	0.004	0.042	0.032	0.010

Table 5.4: Dynamic Roll Angle at Different Speeds (Continued)

	80 km/h			90 km/h			100 km/h		
Radius (m)	Average Observed	Theor-etical	Roll Angle Dynamic	Average Observed	Theor-etical	Roll Angle Dynamics	Average Observed	Theor-etical	Roll Angle Dynamics
873.2	0.024	0.013	0.011	0.040	0.029	0.011	0.043	0.046	-0.003
873.2	0.008	0.005	0.003	0.030	0.020	0.010	0.024	0.037	-0.013
873.2	0.019	0.014	0.005	0.034	0.030	0.005	0.043	0.047	-0.004
873.2	0.020	0.013	0.007	0.038	0.029	0.010	0.054	0.046	0.008
873.2	0.018	0.020	-0.002	0.041	0.035	0.006	0.047	0.052	-0.006
873.2	0.026	0.015	0.011	0.035	0.031	0.005	0.039	0.048	-0.009
873.2	0.023	0.009	0.015	0.037	0.024	0.013	0.051	0.041	0.010
873.2	0.023	0.018	0.006	0.029	0.033	-0.004	0.042	0.050	-0.009
873.2	0.009	0.008	0.001	0.030	0.024	0.006	0.050	0.041	0.009
873.2	0.019	0.013	0.006	0.030	0.028	0.002	0.044	0.045	-0.001
873.2	0.010	0.010	0.000	0.027	0.026	0.001	0.047	0.043	0.004
873.2	0.018	0.008	0.010	0.033	0.024	0.010	0.047	0.041	0.006
873.2	0.039	0.008	0.031	0.035	0.023	0.012	0.025	0.041	-0.015
873.2	0.027	0.000	0.028	0.032	0.015	0.017	0.049	0.032	0.017
873.2	0.016	0.019	-0.003	0.032	0.034	-0.002	0.047	0.052	-0.005
876.0	N/A	N/A	N/A	0.034	0.024	0.010	0.041	0.041	0.000
880.0	N/A	N/A	N/A	0.036	0.020	0.016	0.049	0.037	0.012
900.0	0.011	0.014	-0.003	0.023	0.029	-0.006	0.048	0.046	0.003
900.0	0.010	0.012	-0.003	0.004	0.027	-0.023	0.034	0.044	-0.010
1000.0	N/A	N/A	N/A	0.020	0.016	0.003	0.029	0.031	-0.002
1160.0	N/A	N/A	N/A	0.012	0.009	0.003	0.022	0.022	0.001
1164.0	N/A	N/A	N/A	0.019	0.004	0.015	0.018	0.017	0.001

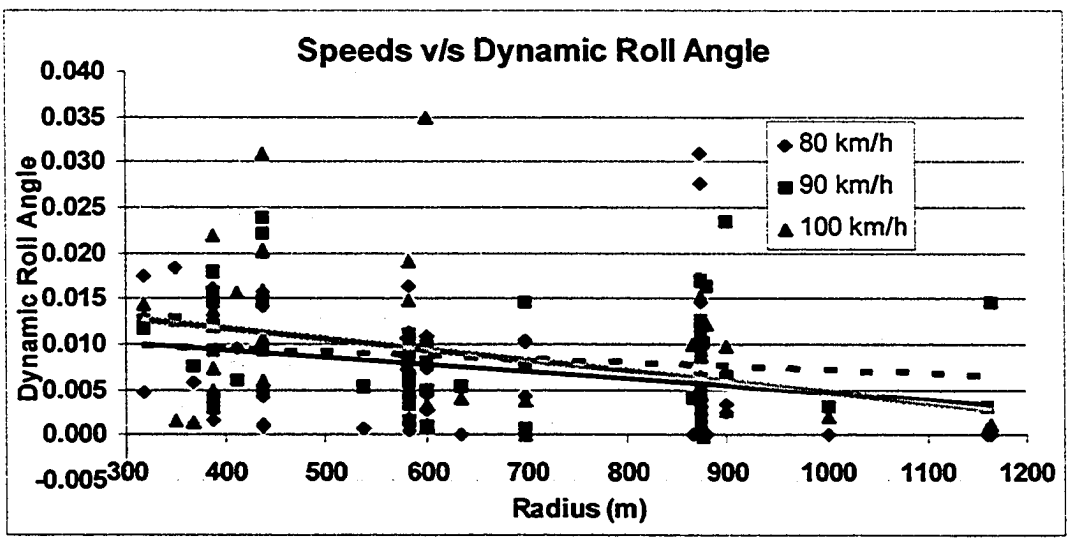

Figure 5.6: Effect of Speeds on Dynamic Roll Angle

These results are showing that there is very slight effect of speeds and radius of curves on dynamic roll angle. Dynamic roll angle values are decreasing with increase in radius of curves and rate of decrease increases with increase in speeds from 80 km/h to 100 km/h. The minimum value of dynamic roll angle is 0 while maximum is 0.035, which shows a change of 2 degrees that is within the limits given in literature review.

5.2.7 ANOVA Test of Dynamic Roll Angle

One-way Analysis of Variance (ANOVA) was carried out to examine the effect of speed on dynamic roll angle and to test the null hypothesis that the mean values of static roll angle corresponding to different driving speeds are equal. Observed *p*-value of dynamic roll angle is 0.094, which is greater than critical value of 0.05. It shows that difference between means is not great enough and hence effect of speed on dynamic roll angle is non-significant. Furthermore, the observed value of *F-ratio* (F_{obs}) is 2.399, which is less than the value of critical *F-ratio* (F_{crit}) i.e. 3.06. Although F_{abs} is less than F_{crit} the difference between two values is very little compared to the difference in the case of static roll, and hence shows some effect of speed on dynamic roll angle compared to static roll. However, from a statistical point of view, the available data suggests that the difference of results may be due to random variation; a finding that may have resulted from the small range of speed data available for analysis.

5.2.8 Models for Average Observed versus Theoretical Lateral Acceleration

Statistical models of relationship between average and theoretical lateral acceleration were developed. Dependent variable considered was average observed lateral acceleration while independent variables were theoretical lateral acceleration and superelevation rate. Two models were developed, the first model was without the value of superelevation rate and the second one included the superelevation (refer to Table 5.5 and 5.6). Second model was showing the higher value of R-square and lower value of standard error. This model explained that difference between average and theoretical values of lateral acceleration is affected by superelevation.

Table 5.5: Model Summary- Roll Angle Dynamic

Model	R	R^2	Adjusted R^2	Std. Error of the Estimate
1	0.968	0.938	0.937	0.0103843
2	0.973	0.947	0.947	0.0095888

a. Predictors: (Constant), Theoretical Lateral Acceleration.

b. Predictors: (Constant), Theoretical Lateral Acceleration, Superelevation Angle (e)

Table 5.6: Coefficients- Average Observed v/s Theoretical Lateral Acceleration

Model		Regression Coefficients		t_{cal}	Sig.
		B	Std. Error		
1	(Constant)	0.005	0.001	3.339	0.001
	Theoretical Lat Acc	0.970	0.019	50.340	0.000
2	(Constant)	-0.020	0.005	-4.245	0.000
	Theoretical Lat Acc	0.941	0.019	50.714	0.000
	e (Radian)	0.532	0.097	5.480	0.000

Dependent Variable: Observed Lateral Acceleration

$$\alpha_{av} = 0.005 + 0.97(\alpha_{th}) \qquad (5.8)$$

$$\alpha_{av} = -0.02 + 0.941(\alpha_{th}) + 0.532(e) \quad (5.9)$$

5.3 Model Development

The Linear regression analysis can be used to predict the lateral acceleration produced in the vehicle with uneven weight. The lateral acceleration can be predicted using a combination of dependent and independent variables. Observed Lateral acceleration was taken as the dependent variable while the independent variables considered are:

- Radius of curve (*R*)
- Driving speed (*V*)
- Length of curve (*L*)
- Superelevation rate (*e*)
- Driving direction as a dummy variable that is equal to 1 if right-turn curves and 0 for left-turn curve.

In addition to independent variables listed above, some combinations of these variables were also used in the modelling, which are: Inverse function of radius (*1/R*) and theoretical lateral acceleration [$a_{th}=(V^2/R)-e$] -function of radius, speed and superelevation rate.

Since, just one vehicle was involved in this study; therefore, values of track width, height of centre of gravity from roll centre, sprung weight of car, roll angle and out side-wheel weight values were constant. These variables are called control or nuisance variables which can be defined as: a variable may affect relationship but of no intrinsic interest in a particular study. Therefore these five variables were not considered in this study. However these variables can be

helpful in determining the predicted values of lateral acceleration if multi vehicles study will be conducted on the same topic in future.

To determine the relationship between dependent and independent variables, they were entered to the Statistical Package for Social Science (SPSS version 13). Several strategies can be used to study the relationship between two variables by means of regression analysis. One of the best is stepwise regression method. This is a modified version of forward regression that permits re-examination, at every step, of the variables incorporated in the model in previous steps (Kleinbaum 1998). Thus those independent variables that are not significant, at the 95% confidence level would be automatically excluded from the model.

5.3.1 Scatter Graphs and Correlations of Coefficients

Scatter graphs of observed lateral acceleration as dependent variable versus all the independent variables individually were drawn and straight-line equation and R-square values were calculated using Microsoft Excel. It was checked if this line best fit to the data available. The correlation coefficient (r) is an often-used statistic that provides a measure of how two random variables are linearly associated in a sample and has properties closely related to those of straight-line regression. The possible values of *"r"* range from –1 to 1 which is dimensionless. Beside positive and negative its value might be zero too. High positive or negative value of "r" shows its stronger positive or negative association with other variable. If value is 1, fit of model is perfect. Scatter graphs of dependent to different independent variables were drawn (refer to Figure 5.7).

Description of the relationship between observed lateral acceleration and each independent variable presented in Figure 5.7 can be stated as follows:

1. Radius of curve: the value of correlation coefficient (r) is –0.53, which indicates a strong negative linear relationship.
2. Theoretical lateral acceleration: the value of correlation coefficient (r) is 0.64, which indicates a strong positive linear relationship.
3. Driving speed: the value of correlation coefficient (r) is 0.26, which indicates a moderate positive linear relationship.
4. Length of curve: the value of correlation coefficient (r) is 0.01, which is close to zero and hence indicates that there is no any linear relationship between the two.
5. Sperelevation rate: the value of correlation coefficient (r) is 0.24, which indicates a moderate positive linear relationship.
6. Inverse function of radius of curve: the value of correlation coefficient (r) is 0.56, which indicates a strong positive linear relationship.

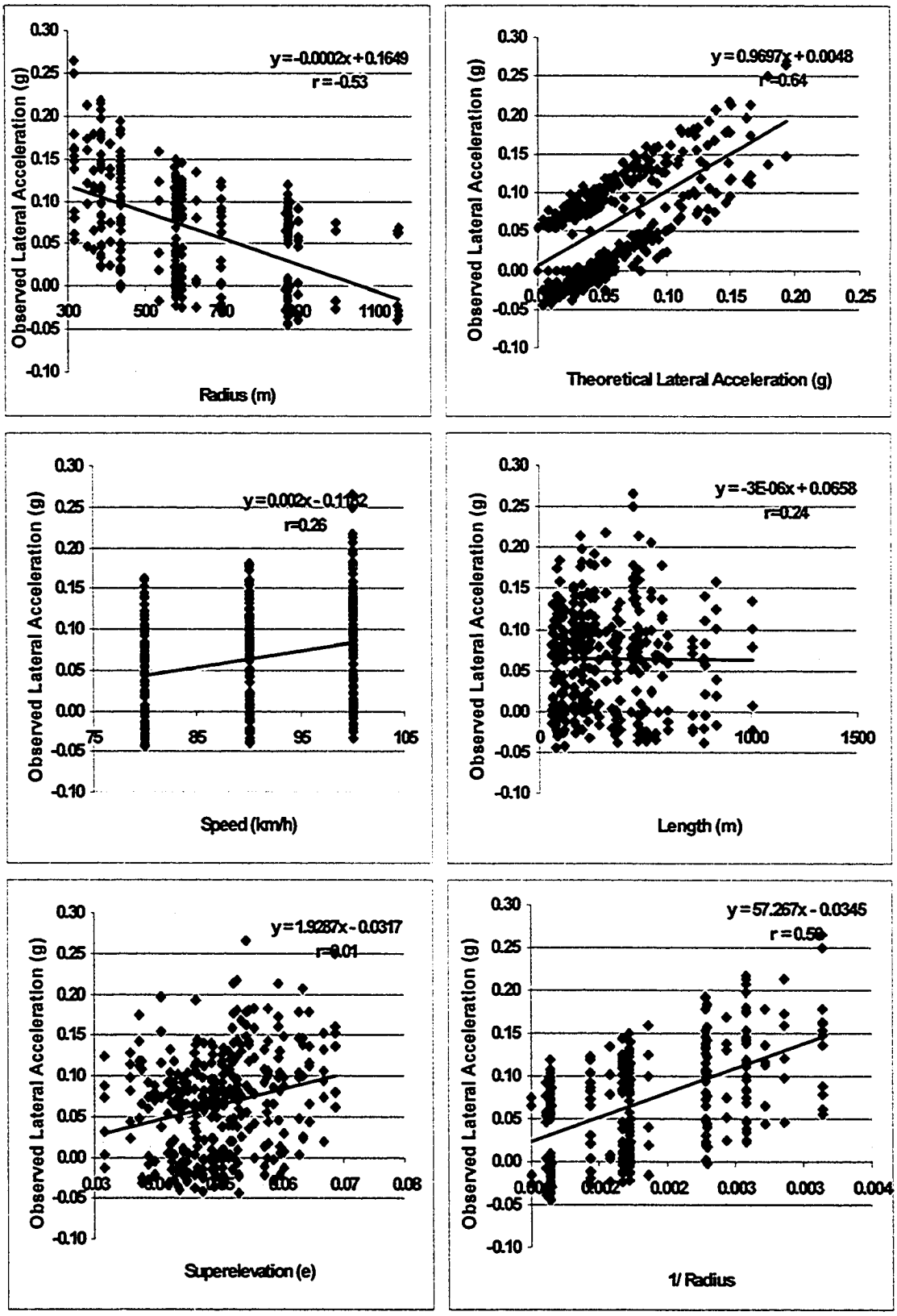

Figure 5.7: Scatter Graphs of Observed Lateral Acceleration v/s Different Independent Variables

To reach to the best-fit line, different options of straight line were tried upon these relationships. Important one is inverse function of radius of curve. Not much success could get except there was slight improvement in value of correlation of coefficient when radius of curve was tried with inverse value (r= 0.56). A graph of relationship between these two variables can also be seen in Figure 5.7. In case of operating speed only three driving speeds were tried. This variable was tried with square function but due to limited number of values no improvement was observed. However, in any future study where different operating speeds will be used this variable can also be used in predicting the value of lateral acceleration with uneven weight. Besides scatter graphs, correlation was also determined through SPSS. Below given Table 5.7 is presenting relationship between different variables. The correlation coefficients values of superelevation, speed, and length with dependent variable are almost similar to the values calculated using Excel. Correlation among the independent variables themselves was also determined. The given below Table 5.7 shows a strongest inverse relationship of correlation between radius and superelevation. Its mean increase in radius of curve will decrease the superelevation rate. Both the Excel and the SPSS show that length of curve does not have any relationship with observed lateral acceleration. Furthermore, speed and superelevation are showing weak relationship.

5.3.2 Selection of Models

A number of models were tried to find out the best representative models for prediction. In first step, all the chosen independent variables were tried in model 1 to 4 (refer to Table 5.7). The independent variables entered were inverse function of radius of curve (*1/R*), speed (*V*), superelevation rate (*e*), length of curve (*L*) and driving direction (*d*). In this first attempt stepwise regression completely excluded length of curve from all models, which also coincide with the results of scatter graphs where correlation coefficient of observed lateral acceleration and length of curve have no any relationship. The last model, which considered all remaining independent variables, was found best due to highest value of coefficient of determination (R^2 = 0.94) and lowest value of standard error (0.0153). The lowest value of standard error shows the closeness of values of observed lateral acceleration about the regression line. Furthermore, the value of adjusted *R*-square is not different from *R*-square, which shows that addition of any new variable in the regression will not make any change in results. This model was chosen for final selection.

Table 5.7: Model Summary (First Attempt)

Model	R	R^2	Adjusted R^2	Std. Error of the Estimate
1	.735(a)	.540	.539	.0425051
2	.925(b)	.855	.854	.0239313
3	.968(c)	.938	.937	.0156878
4	.970(d)	.940	.940	.0153965

a Predictors: (Constant), Driving Direction

b Predictors: (Constant), Driving Direction, 1/Radius

c Predictors: (Constant), Driving Direction, 1/Radius, Speed

d Predictors: (Constant), Direction, 1/Radius, Speed, Superelevation Angle (e)

Table 5.8: Details of Coefficients (First Attempt)

Model	Description	Regression Coefficients		t_{cal}	Sig.
		B	Standard Error		
1	Constant	.019	.003	5.742	.000
	Direction	.092	.005	19.936	.000
2	Constant	-.080	.004	-19.596	.000
	Direction	.092	.003	35.409	.000
	1/Radius	57.267	2.121	27.005	.000
3	Constant	-.284	.010	-28.432	.000
	Direction	.092	.002	54.015	.000
	1/Radius	58.648	1.392	42.142	.000
	Speed	.002	.000	21.171	.000
4	Constant	-.268	.011	-24.933	.000
	Direction	.092	.002	55.037	.000
	1/Radius	61.556	1.574	39.113	.000
	Speed	.002	.000	21.693	.000
	Superelevation	-.453	.122	-3.719	.000

In the second attempt, function of independent variables i.e. theoretical lateral acceleration (a_{th}) along with driving direction (*d*) and superelevation rate (*e*) were tried (refer to Table 5.9). In this attempt two models were found suitable for final selection. These models have highest values of R-square (0.952 and 0.956) and lowest value of standard error (0.0138 and 0.0132). Furthermore, value of adjusted R-square is not significantly different from R-square.

Table 5.9: Model Summary (Second Attempt)

Model	R	R^2	Adjusted R^2	Std. Error of the Estimate
1	.735(a)	.540	.539	.0425051
2	.976(b)	.952	.951	.0137951
3	.978(c)	.956	.955	.0132074

a Predictors: (Constant), Driving Direction

b Predictors: (Constant), Driving Direction, Theoretical Lateral Acceleration

c Predictors: (Constant), Driving Direction, Theoretical Lateral Acceleration, Superelevation Angle (e)

Table 5.10:Detail of Coefficients (Second Attempt)

Model	Description	Regression Coefficients		t_{cal}	Sig.
		B	Standard Error		
1	Constant	.019	.003	5.742	.000
	Direction	.092	.005	19.936	.000
2	Constant	-.041	.002	-26.754	.000
	Direction	.092	.001	61.426	.000
	Theoretical Lateral Acceleration	.970	.018	53.590	.000
3	Constant	-.066	.005	-14.203	.000
	Direction	.092	.001	64.160	.000
	Theoretical Lateral Acceleration	.941	.018	52.071	.000
	Superelevation	.532	.094	5.627	.000

The final three models selected for predicting the lateral acceleration observed with uneven weight of vehicle can be seen in equation 5.10 to 5.12.

$$\alpha_y = -0.268 + 0.092(d) + 61.556(R)^{-1} + 0.002(v) - 0.453(e) \qquad (5.10)$$

$$\alpha_y = -0.041 + 0.092(d) + 0.97(\alpha_{th}) \qquad (5.11)$$

$$\alpha_y = -0.066 + 0.092(d) + 0.941(\alpha_{th}) + 0.532(e) \quad (5.12)$$

where

v = speed (km/h)

α_y = predicted lateral acceleration (g)

d = driving direction

α_{th} = theoretical lateral acceleration (g)

e = superelevation rate (radian)

Chapter 6
Conclusion and Recommendation

6.1 Summary of Study

As documented in the literature, operating speeds of vehicles turning left are more than those turning right in curves with small radius. It was not clear, what makes vehicle to move faster while turning left. The objective of this study was first to determine if uneven weight distribution in vehicles has any effect on lateral acceleration during curve driving at high speeds and large radius of curves. Secondly, to find out how this effect appears in different driving directions i.e. in right and left-turn curves. And finally, to develop models for predicting the lateral acceleration from uneven weight distribution vehicles with respect to other related components of highway curves and vehicle dynamics.

The effect of uneven weight on lateral acceleration and how this weight affects the lateral acceleration in different driving directions was investigated. The methodology included using the lateral acceleration in different directions to calculate the effect of static weight in terms of static roll angle and then investigating the effects of speeds and radius on this value of roll angle. The dynamic roll angle was also calculated and investigated in the same way. In this regard, the driver side (i.e. left side) of the vehicle was kept heavier than the opposite side (i.e. right side)

Seven two-lane rural highways located in Eastern Ontario were chosen for study. Most of the geometric data were provided by MTO and SDG. Research team collected the remaining data, which were related to superelevation, and

vehicle dynamics. Selection criteria were developed to choose adequate curves from these seven highways. To assure the accuracy, two different types of equipment were used for collection of lateral acceleration values while only one vehicle was involved in data collection. Driving speeds were chosen on the basis of a previous study of same curves to ensure that selected speeds are representative of the posted and operating speeds of these highways. The laboratory of Civil and Environmental Engineering, at Carleton University provided technical assistance with manufacturing and purchasing of the instrument required to install and operate data collection equipment.

Data from both types of equipment were carefully screened and formatted. Manufacture assistance was requested whenever needed. During formatting, Microsoft Excel tools were used to calculate the different statistical relationships. Excel tools were also used for formatting graphs to represent the available data. The data collected from right-turn curves were significantly higher than theoretical lateral acceleration i.e. point mass equation. Theoretical lateral acceleration was higher than observed lateral acceleration from left-turn curves. This pattern revealed that static weight on the left side of the vehicle increasing the values of lateral acceleration at right-turn curves and at the same time decreasing in left-turn curves. This point was further investigated and it was discovered that when vehicles negotiate a horizontal curve, lateral forces are developed on the vehicle and driver. The traditional assumption in highway design practice has been that lateral forces and driver's perception of them depend only on the curve radius and rate of superelevation and are independent

of the vehicle characteristics and turning directions. However, if a vehicle is turning right on a superelevated curve, and if the driver side is heavier, the outside wheels will have three types of weights. The first is the weight transferred from the inside wheels due to lateral forces; the second is the weight transferred due to the body roll; and the third force is the available additional static weight on the driver's side. This additional static weight will cause the lateral acceleration to be higher than in the case of a left turn.

This crucial observation was further confirmed by data analysis using two different methodologies. In first method, difference between values in right-turn curves to left-turn curves was calculated. This difference was assumed to be the double of the static roll angle in term of lateral acceleration (one from each direction). This important finding was displayed in both the tabular and the graphical form. In second step dynamic roll angle was also calculated by assuming that difference between average observed to theoretical lateral acceleration is due to the dynamic roll angle. Subsequently, models for predicting the lateral acceleration with uneven vehicle weight were developed by using SPPS. Before model building, relationships between each individual variable and the dependent variable i.e. observed lateral acceleration were investigated. A strong relationship was found between observed and theoretical lateral acceleration. Moreover, a strong relationship existed between curve radius and the dependent variable while a relationship was also observed between superelvation rate and radius of curve. Finally three models on the basis of high

values of coefficient of determination and lowest values of standard errors were selected for predicting the lateral acceleration with uneven weight.

6.2 Conclusion of Study

This research provides evidence that:

- Uneven weight of vehicle causes the static roll angle during curve driving. If higher weight side is at left side of the vehicle; superelevated side is also from left to right and the vehicle is turning right; then the lateral acceleration values of the right side will be higher than left side.
- The observed lateral acceleration of the right-turn curves will be higher than the theoretical lateral acceleration. Conversely, observed lateral acceleration at left-turn curves will be lower than theoretical values of lateral acceleration. The average values of lateral acceleration at right and left-turn curves will be close to the theoretical lateral acceleration.
- The gap between observed lateral acceleration at right-turn curves and theoretical lateral acceleration is unchanged in speeds of 80 km/h and with curve radii ranging from 300 m to 1200 m. The gap between these two values decreases with increase in speeds from 80 to 100 km/h. The gap between observed lateral acceleration at left-turn curves and the theoretical lateral acceleration decreases with increasing speeds from 80 to 100 km/h and curve radii ranging from 300 m to 1200 m.
- The average difference between observed lateral acceleration on right to left-turn curves is close to the twice of value of static roll angle. The

difference between average observed and theoretical lateral acceleration is due to the dynamic roll angle.

- It was observed that speed and radius of curve do not significantly affect the values of static roll angle. Statistical analysis showed that static roll angle values are almost constant for all radii (317 m to 1164 m) and speed of curve (80 km/h to 100 km/h).
- It was observed that speed has some effect on dynamic roll angle as compared to static roll. However, further tests revealed that this effect of speed upon dynamic roll angle is not significant.

6.3 Comments and Proposal for Future Research

During this research many new points were observed. Among them, some are very closely related to the area of this research. However, the limited scope of this study prevented any further investigation of these findings. Any subsequent research may incorporate the above to enhance the understanding in the field. These findings include:

1. The equation used for calculating static roll angle due to uneven vehicle weight does not take into consideration important features like track width, height of centre of gravity of vehicle, and sprung weight. Any future study could develop a new model for calculating the static roll angle to evaluate the impact of these important factors.
2. Since this research involved only one vehicle, it is not appropriate at this stage to generalize the findings in a multiple vehicle scenario. Use of

multiple vehicle for data collection will allow observing the effect of differing values of track width, height of centre of gravity, and sprung mass on lateral acceleration.

3. This study considered the average values of the lateral acceleration. However, peak values of lateral accelerations are also of vital importance. There is need to repeat the same study, while considering the peak values of lateral acceleration of vehicles with uneven weight.
4. The effect of driving directions played and important role in the case of uneven weight. There is need to evaluate the effect of driving directions on lateral acceleration values of vehicles travelling with equally distributed weight.
5. The lateral acceleration values of a vehicle turning right and having uneven weight are much higher than the lateral acceleration of a vehicle having equally distributed weight. There is need to use these higher values due to uneven weight for calculating the new factor of safety against skidding.

References

American Association of Highway and Transportation Officials. 2001. *A Policy on Geometric Design of Highways and Streets,* Washington, D.C.

AutoZine Technical School. 2003. *Lateral Acceleration and Weight Transfer.* http://www.geocities.com/gkurka2001/CarTech/tech handling_3.htm#Weight 20%lateral%20force. Accessed on June 08, 2003.

Baldwin, D. M. 1946. *The Relation of Highway Design to Traffic Accident Experience.* Proceedings of AASHO Convention Group Meeting.

Bonneson, A. J. 1999. Side Friction and Speed as Controls for Horizontal Curves Design. *Journal of Transportation Engineering/November/ December,* 1999, pp 473-480.

Bonneson, A. J. 2000. Kinematics Approach to Horizontal Curve Transition Design. *Transportation Research Record 1737*, pp 1-8.

Bonneson, A. J. 2001. Control of Horizontal Curves Design. *Transportation Research Record 1751*, pp 82-89.

Carlson P.J. and J. M. Mason, Jr. 1999. Relationship Between Ball Bank Indicator Readings, Lateral Acceleration Rates, and Vehicular Body-Roll Rates. *Transportation Research Record 1658*, pp 34-42.

Chowdhury, M. A., Warren, and H. Bissell. 1991. Analysis of Advisory Speed-Setting Criteria. *Public Roads,* Vol. 55(3), Dec 1991, pp 65-71.

Chowdhury, M. A., Warren, Bissell and S. Taori. 1998. Are the Criteria for Setting Advisory Speeds on Curves Still Relevant? *ITE Journal,* Vol. 68(2), Feb. 1998, pp 32-45.

Craus, J. and M. Livneh. 1978. Superelevation and Curvature of Horizontal Curves. *Transportation Research Record 685*, pp 7-13.

Dixon, J. C. 1996. *Tires Suspension and Handling Second Edition.* Society of Automotive Engineers, Inc., Warrendale, PA, USA.

Emmerson, J. 1969. Speed of Cars on Sharp Horizontal Curves, *Traffic Engineering and Control,* Vol. 11, July 1969, pp. 135-137.

Fitzpatrick, K. 1994. Horizontal Curve Design: An Exercise in Comfort and Appearance. *Transportation Research Record 1445*, pp 47-53.

Fitzpatrick, K., Shamburger, Brian and D. Fambro. 1996. Design Speed, Operating Speed and Posted Speed Survey. *Transportation Research Record 1523*, pp 55-60.

Flipe, E. and F. Navin. 1998. Automobiles on Horizontal Curves, Experiments and Observations. *Transportation Research Record 1628*. pp 50-56.

Gillespie, T. D. 1992. *Fundamental of Vehicle Dynamics.* Society of Automotive Engineers, Inc., Warrendale, Pa., USA.

Glennon, J. C. 1987. Effect of Alignment on Highway Safety State of Art Report No. 6 Relationship Between Safety and Key Highway Functions. *Transportation Research Board*, pp 48-63.

Glennon, J .C. and G. D. Weaver. 1983. Highway Curve Design for Safe Vehicle Operations. *Taxes Transport Institute,* pp 15-26.

Harwood, D. W. and M. Mason, Jr. 1994. Horizontal Curve Design for Passenger Cars and Trucks. *Transportation Research Record 1445*, pp 22- 33.

Kleinbaum, D.G., Kupper, Muller and A. Nizam. 1998. *Applied Regression Analysis and Other Multivariable Methods Third Edition,* Duxury Press, CA, USA.

Kneebone, D.C. 1964. Advisory Speed Signs and Their Effect on Traffic. Proc., 2nd Conf., 2(1), *AustraliaN Road Research Board,* Nunawading. 1964, pp 524-538.

Krammes, R. A., Brackett., Shafer., Ottsen., Anderson., Fink., Collins., Pendleton, and C. J. Messer. 1995. *Horizontal Alignment Design Consistency For Rural Two-Lane Highways,* Report FHWA-RD-94-034. FHWA, Washington, US.

Lamm, R., Choueiri and T. Mailaender. 1991. Side friction Demand Versus Side Friction Assumed for Curve Design on Two-Lane Rural Highways. *Transportation Research Record 1303*, pp11- 21.

Leiphart K. L. and K. Epstein. 2002. Spotlight and Safety, *Public Roads,* U.S. Department of Transportation, Federal Highway Administration, Highway Research Centre.

McLean, J. 1983. Speeds on Curves: Side Friction Factor Considerations, *Australian Road Research Board*, Research Report ARR No. 126, pp 1-16.

McLean, J. 1979. An Alternative to the Design Speed Concept for Low Speed Alignment Design. *Australian Road Research Board,* Record 702, pp 55-63.

McLean, J. R. 1974. Driver Behaviour on Curves- A Review, *Australian Research Board,* Vol. 7(5), pp 129-147.

However, further tests revealed that this effect of speed upon dynamic roll angle is not significant.

Merritt, D. R. 1988. Safe Speeds on Curves: A Historical Perspective of the Ball Bank Indicator. *ITE Journal*, Vol. 58(9), September 1988. pp 15-19

Morrall. J.F. and R.J. Talarico. 1994. Side Friction Demanded and Margins of Safety on Horizontal Curves. *Transport Research Record 1435*, pp145-152

Moyer, J. F. and D.S. Berry 1940. Marking Highway Curves With Safe Speed Indicators. Twentieth Annual Meeting. *Transportation Research Board,* Vol. 20, pp 399-428.

National Highway Traffic Safety Administration's Rating System for Rollover Resistance. 2002. *Transportation Research Board Special Report 265*, National Research Council.

Nicholson, A. 1998. Superelevation, Side Friction, and Roadway Consistency. *Journal of Transportation Engineering,* September/October 1998, pp 411-418.

Organization for Economic Cooperation and Development (OECD) Countries. 2002. Report on "*safety on Roads*", what's the vision, OECD, Paris, France.

Peyman, M. 2003. *Modelling Operating Speed and Speed Difference for Design Consistency Evaluation.* Carleton University, Ottawa, Canada.

Reymond, G., Kemeny and A. Droulez. 2001. Role of Lateral Acceleration in Curve Driving: Driver Model and Experiment on a Real Vehicle and a Driving Simulator, *Human Factors*, Fall 2001, pp 484-495

Ritchie, M.L., McCoy and W.L. Welde 1968. A Study of the Relation Between

Forward Velocity and Lateral Acceleration in Curves During Normal, *Human Factors,* 1968, 10 (3), pp 255-258

Salt, G. F. and F. Fice. 1976. Research on Skid-Resistance at the Transport and Road Research Laboratory *Transport Research Record 622*, 1976, pp 26-38

Toyota Reports Record Year-End Result. 2004. *Higher Vehicle Sales in All Regions Play Key Role.* http://www.toyota.cojp/en/news/04/0511.html. Accessed on June 25, 2004.

Appendix A

Appendix A.1: Alignment and Geometric Data for Highway 31 (Speed Limit 80 km/h)

Curve #	Point of Intersection	Radius (m)	Length (m)	Spiral (m)	Superel-vation	Data Collection date and time	Remarks
1	516+50.57	873.20	77.60	60.96	0.044	Oct 15, 03 (11.45 – 14.00)	
2	537+48.61	873.20	76.60	60.96	0.053	Oct 15, 03 (11.45 – 14.00)	
3	583+91.94	873.20	464.20	60.96	0.043	Oct 15, 03 (11.45 – 14.00)	
4	621+53.91	873.20	474.00	60.96	0.044	Oct 15, 03 (11.45 - 14.00)	
5	121+04.34	436.60	162.40	60.96	0.067	Oct 15, 03 (11.45 – 14.00)	
6	12+572.902	580.00	170.00	60.96	0.049	Oct 15, 03 (11.45 – 14.00)	
7	16+551.184	583.00	377.33	60.96	0.057	Oct 15, 03 (11.45 – 14.00)	
8	17+978.435	583.00	783.64	60.96	0.047	Oct 15, 03 (11.45 – 14.00)	
9	26+621.125	549.00	472.38	60.96	0.060	Oct 15, 03 (11.45 – 14.00)	
10	27+731.038	388.08	527.00	60.96	0.064	Oct 15, 03 (11.45 – 14.00)	

Driving speed: 80, 90 and 100 km/hr, Weather: Rainy.

Appendix A.2: Alignment and Geometric Data for Highway 15 (Speed Limit 80 km/h)

Curve #	Point of Intersection	Radius (m)	Length (m)	Spiral (m)	Superel-evation	Data Collection Date and Time	Remarks
1	11+01.695	582.13	165.71	60.96	0.060	Oct 06, 03 (09.00 – 11.00)	
2	16+364.029	873.19	83.34	60.96	0.037	Oct 06, 03 (09.00 – 11.00)	
3	20+705.088	873.19	58.10	60.96	0.042	Oct 06, 03 (09.00 – 11.00)	
4	11+050.986	873.19	281.40	60.96	0.050	Oct 06, 03 (09.00 – 11.00)	
5	17+324.484	600.00	365.70	60.96	0.051	Oct 06, 03 (09.00 – 11.00)	
6	17+882.942	600.00	227.09	60.96	0.047	Oct 06, 03 (09.00 – 11.00)	
7	19+619.382	900.00	234.31	56.00	0.042	Oct 06, 03 (09.00 – 11.00)	
8	20+565.516	900.00	365.02	56.00	0.044	Oct 06, 03 (09.00 – 11.00)	
9	21+383.625	600.00	205.20	59.00	0.051	Oct 06, 03 (09.00 – 11.00)	
10	22+501.418	600.00	155.95	60.96	0.052	Oct 06, 03 (09.00 – 11.00)	

Driving speed: 80, 90 and 100 km/hr, Weather: Cloudy

Appendix A.3: Alignment and Geometric Data for Highway 7 (Speed Limit 80 km/h)

Curve #	Point of Intersection	Radius (m)	Length (m)	Spiral (m)	Superel-evation	Data Collection date and time	Remarks
1	12+782.386	873.19	726.24	57.98	0.040	Oct15, 03 (16.00-18.00)	
2	10+484.786	873.19	501.10	60.96	0.049	Oct15, 03 (16.00-18.00)	
3	16+501.665	873.19	462.57	60.96	0.045	Oct15, 03 (16.00-18.00)	
4	15+805.846	698.55	340.60	60.96	0.045	Oct15, 03 (16.00-18.00)	
5	15+003.084	410.91	455.37	60.96	0.054	Oct15, 03 (16.00-18.00)	
6	14+304.340	873.19	116.46	60.96	0.047	Oct15, 03 (16.00-18.00)	
7	13+963.290	582.13	66.450	60.96	0.042	Oct15, 03 (16.00-18.00)	
8	13+063.321	582.13	75.45	60.96	0.052	Oct15, 03 (16.00-18.00)	
9	11+687.846	582.13	199.22	60.96	0.060	Oct15, 03 (16.00-18.00)	
10	10+114.883	436.59	105.67	60.96	0.049	Oct15, 03 (16.00-18.00)	

Driving speed: 80, 90 and 100 km/hr, Weather Rainy.

Appendix A.4: Alignment and Geometric Data for Highway 17 (Speed Limit 90 km/h)

Curve #	Point of Intersection	Radius (m)	Length (m)	Spiral (m)	Superel-evation	Data Collection date and time	Remarks
1	10+794.123	873.00	656.39	60.96	0.010	Oct 16, 03 (12.30- 14.30)	Constructio n on the Road
2	27+042.694	1166.5	821.42	76.20	0.044	Oct 16, 03 (12.30- 14.30)	
3	20+347.506	993.00	544.07	76.20	0.048	Oct 16, 03 (12.30- 14.30)	
4	22+700.738	1000.0	170.91	76.20	0.047	Oct 16, 03 (12.30- 14.30)	
5	254+49.29	582.12	101.60	76.20	0.048	Oct 16, 03 (12.30- 14.30)	
6	262+51.60	582.12	110.91	76.20	0.052	Oct 16, 03 (12.30- 14.30)	
7	297+20.01	436.59	259.08	76.20	0.051	Oct 16, 03 (12.30- 14.30)	
8	313+91.55	436.59	263.65	76.20	0.046	Oct 16, 03 (12.30- 14.30)	
9				76.20	0.059	Oct 16, 03 (12.30- 14.30)	

Driving speed: 90, 100 and 110 km/hr, Weather: Cloudy.

Appendix A.5: Alignment and Geometric Data for Highway 43 (Speed Limit 80 km/h)

Curve #	Point of Intersection	Radius (m)	Length (m)	Spiral (m)	Superel-evation	Data Collection date and time	Remarks
1	115+82.16	873.19	604.65	60.96	0.049	Oct 01, 03 (11.00-12.00)	
2	220+46.43	388.00	203.99	60.96	0.041	Oct 01, 03 (11.00-12.00)	
3	237+45.38	388.00	240.00	60.96	0.055	Oct 01, 03 (11.00-12.00)	
4	254+49.29	582.12	101.60	60.96	0.053	Oct 01, 03 (11.00-12.00)	
5	262+51.60	582.12	110.91	60.96	0.036	Oct 01, 03 (11.00-12.00)	
6	297+20.01	436.59	259.08	53.34	0.046	Oct 01, 03 (11.00-12.00)	
7	313+91.55	436.59	263.65	53.34	0.063	Oct 01, 03 (11.00-12.00)	

Driving speed: 80, 90 and 100 km/hr, Weather: Sunny

Appendix A.6: Alignment and Geometric Data for Highway 12 (Speed Limit 80 km/h)

Curve #	Point of Intersection	Radius (m)	Length (m)	Spiral (m)	Superelevation	Data Collection date and time	Remarks
1	110+87.82	367.65	579.98	0.00	0.065	Oct 01, 03 (03.00-05.00)	
2	232+09.23	388.08	124.86	0.00	0.060		Interruption on Curve # 2 to 5 due to traffic jam Slow moving vehicles, school activities and Temporary markets.
3	239+82.24	388.08	128.07	0.00	0.049		
4	38+51.72	698.55	352.96	0.00	0.043		
5	79+33.66	436.59	233.04	0.00	0.042		
6	239+30.10	698.55	121.92	0.00	0.032		
7	246+37.77	698.55	113.49	0.00	0.043		
8	286+90.81	317.52	443.34	0.00	0.055		
9	305+58.89	317.52	445.47	0.00	0.069		

Driving speed: 80, 90 and 100 km/hr, Weather Partly Cloudy

Appendix A.7: Alignment and Geometric Data for Highway 41 (Speed Limit 80 km/h)

Curve #	Point of Intersection	Radius (m)	Length (m)	Spiral (m)	Superel-evation	Data Collection date and time	Remarks
1	126+90.93	388.00	159.79	60.96	0.066	Oct 09, 03 (11.00-14.00)	Busy intersection
2	136+93.09	582.12	110.91	60.96	0.038	Oct 09, 03 (11.00-14.00)	Busy intersection
3	205+35.50	873.19	430.66	45.72	0.050	Oct 09, 03 (11.00-14.00)	
4	256+68.03	873.19	208.79	45.72	0.058	Oct 09, 03 (11.00-14.00)	
5	336+30.65	806.00	541.13	45.72	0.040	Oct 09, 03 (11.00-14.00)	Road construction
6	356+86.57	582.12	71.12	45.72	0.046	Oct 09, 03 (11.00-14.00)	
7	382+00.02	436.59	100.14	45.72	0.056	Oct 09, 03 (11.00-14.00)	
8	397+06.63	436.59	204.66	45.72	0.058	Oct 09, 03 (11.00-14.00)	
9	11+915.302	388.08	314.23	60.96	0.053	Oct 08, 03(11.00-15.00)	
10	15+238.372	873.19	358.18	60.96	0.039	Oct 08, 03(11.00-15.00)	
11	16+570.919	388.08	194.96	60.96	0.052	Oct 08, 03(11.00-15.00)	
12	17+031.136	1164.25	226.91	60.96	0.035	Oct 08, 03(11.00-15.00)	Built-up area
13	18+188.717	388.08	87.99	60.96	0.037	Oct 08, 03(11.00-15.00)	
14	20+886.703	436.59	53.02	60.96	0.055	Oct 08, 03(11.00-15.00)	Built-up area
15	26+043.167	537.35	836.90	60.96	0.052	Oct 08, 03(11.00-15.00)	
16	27+621.685	635.05	1001.9	60.96	0.051	Oct 08, 03(11.00-15.00)	

Driving speed: 80, 90 and 100 km/hr, Weather Sunny